공학박사 학위논문

Water Motion Active Transducer for Energy Harvesting

물의 움직임을 이용하는 능동형 트랜스듀서의 에너지 하베스팅 적용 연구

2017년 2월

서울대학교 대학원

융합과학부 나노융합전공

권 순 형

Water Motion Active Transducer for Energy Harvesting

지도교수 김 연 상

이 논문을 공학박사 학위논문으로 제출함
2016년 11월

서울대학교 대학원
융합과학부 나노융합전공
권 순 형

권순형의 박사학위논문을 인준함
2016년 12월

위 원 장 박 원 철 (인)

부 위 원 장 김 연 상 (인)

위 원 김 영 훈 (인)

위 원 이 정 노 (인)

위 원 한 철 종 (인)

Abstract

Water Motion Active Transducer for Energy Harvesting

Soon-Hyung Kwon
Program in Nanoscience and Technology
The Graduate School of Convergence Science and Technology
Seoul National University

As effective methods to convert mechanical motion to electrical power, various transducers, such as electromagnetic inductive transducers, piezoelectric transducers, and variable capacitive transducers have been developed. The electromagnetic inductive transducers defined by Faraday's law are predominantly used for electric energy harvesting from mechanical motion. Furthermore, the piezoelectric transducers are becoming an emerging technology for self-powered portable devices. Otherwise, in spite of the potential for energy transducing by variable capacitance, it remains in an infant state for energy harvesting, because it needs additional external bias-voltage sources for the accumulation of charge at the electrodes, which requires a passive transducer, or toxic liquid metals for effective induction. Also, their sources for energy harvesting are

restricted only to artificial intermittent stimulation, like pushing or vibration. To overcome the limitations, I propose a water active capacitive transducer (WMAT) as an energy harvester to effectively generate electric power from the natural motion of water without any external bias voltage sources. One of the most significant limitations in applying capacitive transducers as energy harvesters is that they need an external bias-voltage source to accumulate charge at the electrodes. In my research, two types of WMAT devices are proposed according to various applications. First, I designed the WMAT with a simple structure consisting of PVP dielectric layer, hydrophobic layer on the rigid substrate. This simple structure has considerable advantages for the process and manufacturing cost. All fabrication processes for the WMAT were solely conducted by solution processes without any vacuum or high-cost processes. Second, I introduced a fabric-based WMAT using fabric materials with flexible and stretchable for wearable electronics. In this experiment, core materials for electrification and EDL to generate the electricity are PVP and PMMA energy conversion layers. I studied an effective fabrication method using newly adopted fabric-based materials and polymer materials to find easy and simple method differ from the conventional complex process. Furthermore, I carried out spray coating and transfer process with fabric material to overcome the limitation of spin coating and lithography process of high temperature and chemical treatment. The simple and low-cost process is the most attractive of all of the advantages of the WMAT in comparison to

other energy harvesters with complex structures and cumbersome processes. With variation of the overlapping areas between the water and electrodes, this energy transducer could sufficiently convert the energy from the water's mechanical motion to electric energy. From a simple structure, we successfully generated electricity enough to turn on an LED using various kinds of natural water motion. The WMAT, which has wide applicability, has good potential to be a candidate for generating sustainable electric energy.

Keywords : variable capacitance, energy harvesting, self-powered device, active transducer, water motion, energy conversion

Student Number : 2012-30691

Contents

List of Tables and Figures

List of Publications

1. **Soon-Hyung Kwon**, Junwoo Park, Won Keun Kim, YoungJun Yang, Eungkyu Lee, Chul Jong Han, Si Yun Park, Jeongno Lee and Youn Sang Kim, "An effective energy harvesting method from a natural water motion active transducer", Energy Environ Sci, 7(10), 2014, 3279-3283.
2. Park, J, Yang, Y, **Kwon, S. H**, Kim, Y. S, "Influences of Surface and Ionic Properties on Electricity Generation of an Active Transducer Driven by Water Motion", J. Phys. Chem. Lett, 6, 2015, 745−749.
3. Yang, Y, Park, J, **Kwon, S. H,** Kim, Y. S, "Fluidic Active Transducer for Electricity Generation", Sci. Rep, 5, 2015, 15695.
4. **Soon-Hyung Kwon**, Won Keun Kim, Junwoo Park, YoungJun Yang, Byungwook Yoo, Chul Jong Han and Youn Sang Kim "Fabric Active Transducer Stimulated by Water Motion for Self-Powered Wearable Device", ACS Appl Mater Interfaces, 8(37), 2016, 24579-24584.

Abbreviations

AC	Alternating Current
AFM	Atomic Force Microscopy
Al_2O_3	Aluminum Oxide
$BaTiO_3$	Barium Titanate
DC	Direct Current
EDL	Electrical Double Layer
EH	Energy Harvesting
ITO	Indium Tin Oxide
MEMS	Micro-Electro-Mechanical System
NI	National Instruments
P&O	Perturb & Observe
PEH	Piezoelectric Energy Harvester
PET	Polyethylene Terephthalate
PMMA	Poly(methylmetharylate)
PTFE	Polytetrafluoroethylene
PVDF	Polyvinylidene Fluoride
PVP	Poly-4-Vinyl Phenol
PZT	Lead Zirconium Titanate
STM	Scanning Tunneling Microscopy
TEG	Thermoelectric Generator

TENG	Triboelectric Nanogenerator
TiO_2	Titanium Oxide
WMAT	Water Motion Active Transducer
ZrO_2	Zirconium Oxide

Chapter 1. Introduction

1.1 Introduction

In nature there are a lot of energy resources which could be converted to usable energy form.[1] Past few decades men use hydropower of rivers and ocean to generate electricity, and men also add solar and wind energy to generate electricity in recent years.[2] Availability of hydropower is limited, because there is limited number of dams and environmentally harmful to the nature. Hydropower energy conversion efficiency is rather very low due to the low energy conversion efficiency of mechanical devices such as turbine and solar and wind energy could provide the electricity only intermittently depending upon weather conditions of the locations.[3,4] Lately scientists and engineers are developing new technologies to harvest waste energy using thermoelectricity, piezoelectricity or reverse electrowetting but they are struggling with low energy conversion efficiency and low electric power generation of these devices.[5,6,7] These devices need specific structure and condition to generate the electrical energy. So these devices have the limitation of power generation scale compare to the hydropower generator which generate the electricity from constant and abundant energy source as mentioned.[8] Here we propose a new revolutionary energy concept to generate the electricity using renewable natural energy resource of river stream and ocean current which is predictable and consistent without any harmful by-products such as CO_2 or greenhouse

emission. This technology can generate the electricity under various condition which change the contact area between water and dielectric layer. This simple operating principle can this device to apply water vibration, water flow, water drop, water wave which is common phenomenon in our surroundings. This technology have a simple structure consist of dielectric layer on indium tin oxide (ITO) electrode substructure, water and counter electrode substrate easy scale up having high electrical power generation using array and stacking method.

In chapter 3, I proposed a new concept to generate electricity from water's natural motion without any cumbersome conversion parts or external sources. I found that the overlap area variation between the water and the dielectric layer can effectively induce the variation of electric charges, and then easily generate electricity. The suggested hydroelectric energy harvester which is based on the difference of overlap areas variation between water and electrodes has a simple structure: substrate including the patterned transparent electrodes, poly-4-vinyl phenol (PVP) dielectric layers, and hydrophobic layers. This simple structure in the new hydroelectric energy harvester makes it possible to easily produce electricity from various natural water phenomena in our surroundings, such as rain, rivers, and even sea waves. I achieved electrical power generation of 3.1 V and 5.3 μA from the flowing of the only one tap-water droplet of 30 μL, and successfully turned on light emitting diodes (LED) with natural mimetic water movements, via the suggested hydroelectric energy

harvester. As these new hydroelectric energy harvesters can easily be extended to scale-up power production by the simple stack or array process and have a wide applicability range in hydroelectric generation. This work have been published as "An effective energy harvesting method from a natural water motion active transducer" by Soon-Hyung Kwon, Junwoo Park, Won Keun Kim, YoungJun Yang, Eungkyu Lee, Chul Jong Han, Si Yun Park, Jeongno Lee and Youn Sang Kim, Energy Environ. Sci, 7, 2014, 3279.

In chapter 4, our new fabric-based water motion active transducer (WMAT) was reported. Here, I proposed fabric-based water motion active transducer (WMAT) which has an excellent electrical output using natural water motion like rain for innovative umbrella of self-powered lighting. In this research, I studied the principle of electricity generation from electrical double layer (EDL) between newly adopted fabric electrode and polyurethane-poly methyl-methacrylate (PMMA) layer. Furthermore, I specially carried out spray coating and transfer process with fabric based material to overcome the limitation of spin coating and lithography process of high temperature and chemical treatment. I verified polyurethane-PMMA layer with spray coating process are effective dielectric layer and energy conversion layer on the fabric substrate. To achieve final demonstration, fabric WMAT was detached from glass substrate after core process and was attached to polyester substrate of umbrella surface using transfer process. Unlike the other complex and sensitive energy harvesting devices, our fabric WMAT

has an advantage of physical bending and folding characteristic because all materials are flexible and foldable fabrics. Fabric WMAT has a similar structure with our previous glass-based WMAT but core material is changed suitable for fabric-based process.[9] The main principle of our fabric WMAT is based on electrical double layer (EDL) between PMMA energy conversion layer and water droplet.[10] Water droplet on energy conversion layer is charged with positive polarity due to the asymmetric molecular structure of PMMA with negative polarity.[11] Charged water droplet induces capacitance variation with each electrode and contributes generating electricity. Finally, we realized fabric-based WMAT using spray coating and transfer process of easy and cheap without photo-lithography process of high cost. I achieved the electricity with a peak voltage of 9 V and peak current of 50 μA enough to turn on a green LED using a water droplet of about 30 μL. This work have been published as "Fabric Active Transducer Stimulated by Water Motion for Self-Powered Wearable Device" by Soon-Hyung Kwon,Won Keun Kim,Junwoo Park,YoungJun Yang,Byungwook Yoo, Chul Jong Han and Youn Sang Kim, ACS Appl. Mater. Interfaces, 8(37), 2016, pp 24579-24584.

Finally, chapter 5 summarizes the overall conclusion of this dissertation and describes further research opportunities and applications of energy harvesting using water droplets.

1.2 References

1. Arnold D. P, "Review of microscale magnetic power generation", IEEE Trans. Magn, 43, 2007, 3940-3951.
2. Stephen N. G, "On energy harvesting from ambient vibration", IEEE J. Sound Vib, 293, 2006, 409-425.
3. Frey, Gary W, and Deborah M. Linke, "Hydropower as a renewable and sustainable energy resource meeting global energy challenges in a reasonable way", Energy policy, 30(14), 2002, 1261-1265.
4. Gaden, David LF, and Eric L. Bibeau. "Increasing Power Density of Kinetic Turbines for Cost-effective Distributed Power Generation", Power-gen, April, 2006, 10-12.
5. Stordeur, Matthias, and Ingo Stark. "Low power thermoelectric generator-self-sufficient energy supply for micro systems", Thermoelectrics, 1997, Proceedings ICT'97. XVI International Conference on IEEE.
6. Fang, Hua-Bin, "Fabrication and performance of MEMS-based piezoelectric power generator for vibration energy harvesting", Microelectronics J, 37(11), 2006, 1280-1284.
7. Krupenkin. Tom, and J. Ashley Taylor, "Reverse electrowetting as a new approach to high-power energy harvesting", Nat Commun, 2, 2011, 448.
8. Zhu. Guang, "Toward large-scale energy harvesting by a nanoparticle-enhanced triboelectric nanogenerator", Nano Lett,

13(2), 2013, 847-853.

9. Park Steve, Michael Vosguerichian, and Zhenan Bao. "A review of fabrication and applications of carbon nanotube film-based flexible electronics", Nanoscale, 5(5), 2013, 1727-1752.

10. Park, J, Yang, Y, Kwon, S. H, Kim, Y. S, "Influences of Surface and Ionic Properties on Electricity Generation of an Active Transducer Driven by Water Motion", J. Phys. Chem. Lett, 6, 2015, 745－749.

11. Grahame, D. C, "The Electrical Double Layer and The Theory of Electrocapillarity", Chem. Rev, 41, 1947, 441－501.

Chapter 2. Literature Review

2.1 Energy Harvesting Technologies

Energy harvesting or energy scavenging means the method that collects small energy which would be consumed by heat, light, sound, vibration or movement from ambient environments.[1] Energy harvesting has an advantage for low-power consumption applications such as portable equipment, small consumer electronics, wearable gadget and telecommunication product.[2] Energy harvesting also has a important alternative means for backup battery of various applications, especially its installation place is far from a living space.[3] The source of energy for energy harvesting are various types such as light, heat, peak power and vibration but most of them are not suitable for practical purpose.[4-6] So we understand that the energy harvesting or scavenging process from specific natural and artificial phenomenon is free energy. For examples, we can collect the mechanical energy from vibration, push and strain, thermal energy from the surface of exhaust pipe and engine of automobile and other heating sources.[7-10] Also fluidic energy is induced by from air and various liquid flows. The history of energy harvesting is derived from windmill and waterwheel of our ancestor.[11] People have investigated proper methods of generating electricity from heat, vibration and natural flow for many decades. Many significant experiments in the field of energy harvesting were carried out in the 19th century. In 1821, Thomas Johann Seebeck first found a thermal difference from

two different conductors generate a voltage.[12,13] In 1834, French scientist Jean Charles Athanase Peltier discovered new phenomenon about flowing an electric current from the junction of two different conductors, known as p-type semiconductor and n-type semiconductor, control it to act as a heater or cooler.[14] In 1880, Pierre Curie and Jacques Curie made the concept of piezoelectric effect.[15,16] The concept of tribo-effect dates back to time of the ancient Greeks but the application for energy harvesting device was firstly demonstrated in 2012.[17] These various technologies above mentioned have been maturated by many scientists and engineers eager to apply for practical use in the 21th century. Recent, energy harvesting technology come to the issue novel alternative for new innovative products which are smaller and low powered autonomous system. From one year to another, our battery dependency of portable electronics is growing and rising. The expansion of battery capacity is not the only solution for real nomadic system.[18] To overcome this issue, energy harvesting technology is needed and there are numerous smart device needed for only from 0.1 to few micro-watt level such as pollution sensor, traffic congestion control device, fire detection sensor, smart park system, water quality alarm device and golf course condition check sensor. Energy harvesting has possibility to achieve the electrical energy from almost any environment. These technologies show the tendency of increase the capability for the application in the home, office, road and military use of perpetual or near-perpetual system.

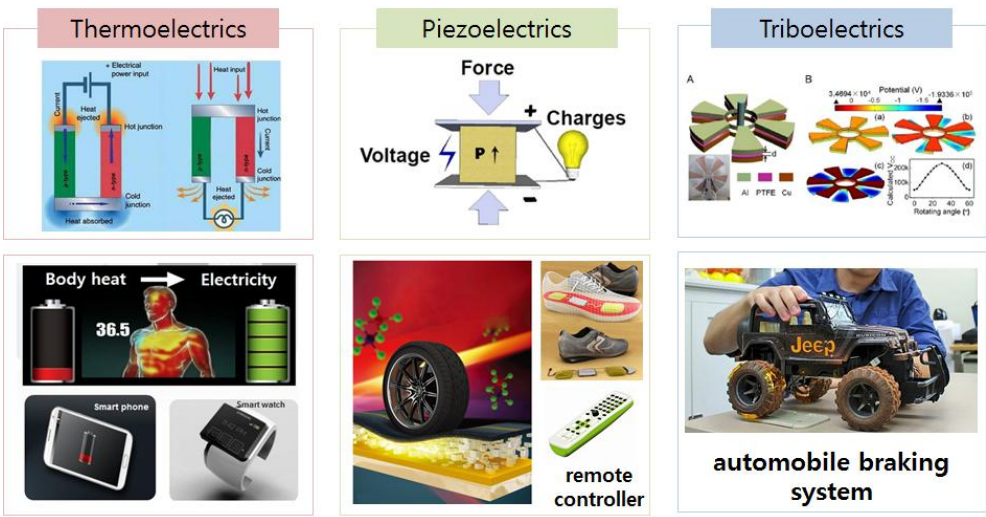

Figure 1. Various energy harvesting technologies for practical purpose.

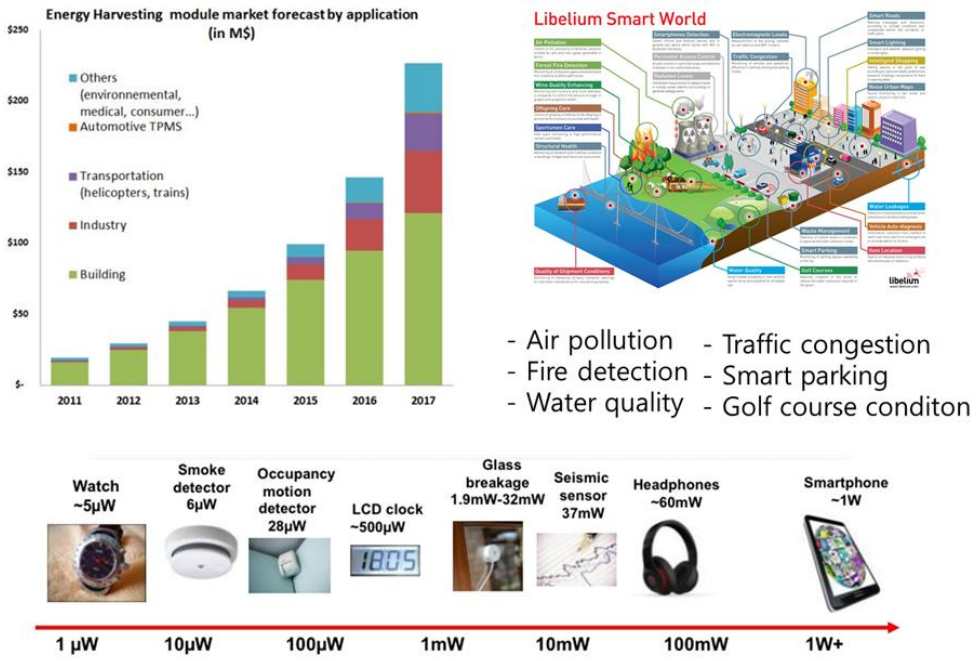

Figure 2. Market forecast by applications of energy harvesting device.

2.1.1 Piezoelectrics

Working Principle and application

Piezoelectricity is a kind of electric charge accumulated by outside stimulation. The meaning of piezoelectricity is electricity result from pressure. The origin of a piezoelectricity is derived from the Greek which means to squeeze or press. Piezoelectric materials are no inversion symmetry that make electrical charges owing to external stress or pressure changing their dipole moment. On the contrary, piezoelectric materials show the reverse effect of wisting or bending when certain voltage is applied to the surface shown in Figure 3. For instance, lead zirconate titanate (PZT) material is known as suitable material for ultrasonic application because its deformation is linear according to the applied voltage.[19] This material shows linear dimension variation 0.1 % compare to its original dimension. This piezoelectric effect is the linear electro-mechanical interaction between mechanical force and electron state of the specific crystalline materials.[20] Piezoelectricity is widely used for various fields of medical device, speaker, ultrasonic nozzle, frequency generator and auto focusing actuator. Moreover, its outstanding merit is exposed to the field of scientific instrumental analysis. The most of the scanning probe microscopies such as scanning tunneling microscopy (STM) and atomic force microscopy (AFM) rest on the basic principle of piezoelectricity. General consumer goods from cigarette lighter, quartz watch and sound effect speaker are also the basis of its principle.

Technologies trends for energy harvesting device

General piezoelectric energy harvesting device have the merit of quick response with peak type electrical power generation. But piezoelectric material is restricted by its own characteristic depend on the inherent structure according to specific frequency variation. This limitation limits the use of piezoelectric energy harvesters in practical life. Many research groups have studied about a cantilerver type piezoelectric energy harvesting device to solve the low power output issue. They anticipate this device has the structure to obtain the high power output because its element is suitable for apply large stress and deformation. Figure 4 show the schematic of cantilever type piezoelectric energy harvesting device. The analysis of electrical characterization is measured by a function generator and an amplifier. In piezoelectrics, core material is the most important factor to improve the output performance. Kim's research team reported a unimorph cantilever with PZT thick layers for energy harvesting device. Cr and Nb co-doping in the PZT materials showed electrical power of 17.3 mW (2.08 mW/cm^3) at 20 Hz.[21] Choi et al. presented experimental results about the relationship between the piezoelectric properties and the output power. They achieved the electrical power of 231 mW/cm3 from the piezoelectric cantilever at 84 Hz under 1 g using modified PZT ceramics with $Pb[(Zn_{0.4}Ni_{0.6})_{1/3}Nb_{2/3}]O_3$ (PZNN).[22] Kim's group investigated the relationship between operation temperature and output power.[23] Song et al. reported the single crystal piezoelectric materials including 0.7 Pb ($Mg_{1/2}Nb_{2/3}$)

O_3-0.3$PbTiO_3$ (PMN-PT) single crystals oriented along the <110> and <001> directions. The maximum power was 1.07 mW at 89 Hz under 0.53 g. Karami's research group studied unimorph cantilever type energy harvesters with single crystal PMN-PZT and showed the maximum output from the cantilever was 226 μW/g^2 at 819 Hz.[24]

Berdy's group modified the natural frequency of piezoelectric device and demonstrated electrical output power was 118 μW at 49.7 Hz of natural frequency under 0.2 g.[25] Shindo et al. also reported output power of 8.5 mW/cm3 at 40 Hz under 3.2 g using a S-shape cantilever.[26] Sobocinski et al. proposed the concept of the wideband piezoelectric energy harvester with a low temperature co-fired ceramic (LTCC) technique. The maximum power output was 32 μW 1100~1165 Hz under 1 g acceleration.[27]

Bulk Piezoelectric Energy Harvesters is another promising candidate of energy harvesting fields. Palosaari et al. proposed cymbal type piezoelectric energy harvester with 0.31 mW/cm^3 at 1.19 Hz compression frequency with 24.8 N force.[28] Chen et al. reported clamped piezoelectric structure device of the electrical power of 12 mW at 113 Hz under 1 g.[29] Tire pressure measurement systems (TPMS) is practical area of battery free device with stacked piezoelectric bending elements by Makki et al.[30]

The MEMS technology is also one of the prospective field to rigid piezoelectric energy harvesting devices. The cantilever method above mentioned is the base technology to obtain the high power output relatively using MEMS piezoelectric harvesters.[31-34]

The structure of MEMS cantilever is similar to the bulk type energy harvesting device.[35] The main materials are consist of Si and metal. Kim's research group reported modified bimorph PZT cantilever. The average power is 9.6 (d31 bimorph) nW at 89.4 Hz.[36,37] Power of MEMS cantilever is depend on the electrode configration and poling direction. Tang et al. reported a PZT microstructure using bulk ceramics.[38] This results show the output voltage of about 1 V at the resonance frequency at 1 kHz using patterned ceramics.[39] Kuehne et al. demonstrated a unique MEMS generator of fluid-actuated energy transducer.[40] The maximum energy density value was 35 nJ/mm2. Lin et al. developed a piezoelectric micro energy harvester using a high-quality PZT. The maximum output power of 200.28 μW at 112.4 Hz.[41] Liu et al's piezoelectric MEMS energy harvester played a role as bridge to increased output power. The resonance frequency of the MEMS generator showed about 36 Hz due to the Si mass structure. Measured maximum output power was from 32.3 nW to 85.5 nW within the operation bandwidth from 30 Hz to 47 Hz.[42,43]

Many scientists related with this area have studied the solution using both two method frequency tuning and bandwidth broadening. A number of research group presented the paper of frequency tuning and broadening for energy harvesting. Frequency tuning means mechanical and electrical method. Also, bandwidth broadening means linear and non linear method.

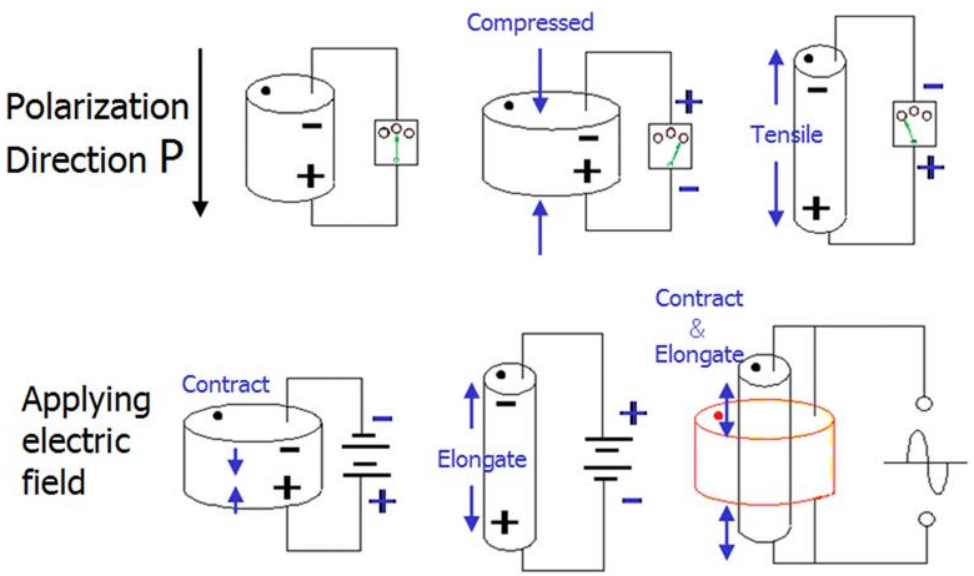

Figure 3. Mechanical - Electrical energy conversion in piezoelectric materials.

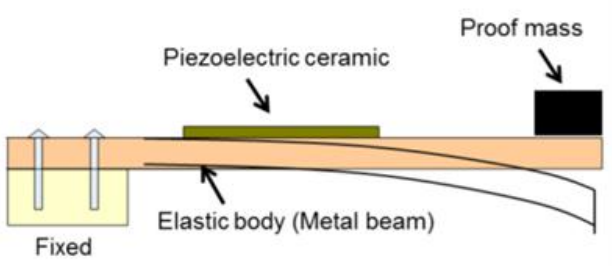

Figure 4. Schematic of cantilever type piezoelectric energy harvesting device. (Reference 21)

Structure	Power Density (mW/cm^3)	Normalized Power (mW/g^2)	Frequency (Hz)
Cr and Nb doped PZT cantilever	2.1	1.1	20
PZNN cantilever	231	11.7	84
<110> oriented single crystalline PMN-PT cantilever	-	3.8	84
<001> oriented single crystalline PMN-PT cantilever	-	1.4	86
PMN-PZT single crystalline cantilever	-	0.2	819
Meandering structured cantilever	0.2	2.9	50
S-shape bulk cantilever	8.5	-	40
Wideband LTCC cantilever arrays	-	0.03	1100–1165

Table 1. Comparison of the output performance of the cantilever type bulk piezoelectric energy harvesting device. (Reference 22-30)

Structure	Power Density ($\mu W/cm^3$)	Normalized Power ($\mu W/g^2$)	Frequency (Hz)
Unimorph cantilever (d_{31} mode)	-	0.0061	89.4
Unimorph cantilever (d_{33} mode)	-	0.0335	89.4
Bimorph cantilever (d_{31} mode)	-	0.015	89.4
Bimorph cantilever (d_{33} mode)	-	0.035	89.4
Micro-cantilever using bulk PZT	28,856	11.6	520
Metal-based MEMS cantilever	98	15.4	89
Metal-based MEMS cantilever	15,453	89.0	112.4
Wideband cantilever	-	0.032–0.085	30–47
S-shape MEMS cantilever	-	0.31	27.4

Table 2. Comparison of the output performance of the microelectro-mechanical systems (MEMS) piezoelectric vibration energy harvesters. (Reference 31-43)

2.1.2 Triboelectrics

Working Principle and application

The mechanism of triboelectricity is based on the contact electrification between two materials which have not equal Fermi level. When certain material contacts with another material, there is happened to lack or excess of electrons. For example, rubbing glass with fabric or hair, produce the triboelectricity. The origin of a word of tribo come from the Greek refers to friction. In 1757, John Carl Wilcke reported the first triboelectric series.[44,45] A lot of materials are arranged in order of polarity according to touch experiment with reference object. They also found, some materials could exchange ions from their surface to another surface. Today, triboelectricity is the target to remove because of its discharges causing from damage in electronic industry, human life and powder production.[46] Triboelectric effect is known as a kind of chemical reaction of two materials which are composed of different molecules.[47,48] This structure is similar to a chemical bond from a point of view electron exchange. Energy harvesting technology using triboelectric effect is realized in the beginning of 21th century. Triboelectric nanogenerator (TENG) is introduced by Wang's research team. The basic operation principle is capacity variation from triboelectricity effect above mentioned. TENG model is classified with 4 models.[49-52] First dielectric to dielectric contact model is expressed in Figure 6(a). The gap distance of two dielectric plates are changed when external force

is applied. Where, d_1 and d_2 is thicknesses, ε_{r1} and ε_{r2}, is respectively relative dielectric constants. When two dielectric plates are contact, electrons transfer phenomenon is happen between the interface of two materials. This relationship is expressed as :

$$V = -\frac{Q}{S\varepsilon_0}(d_0 + x(t)) + \frac{\sigma x(t)}{\varepsilon_0} \quad (1)$$

Where, d_0 is the effective thickness, ε_0 is the dielectric constant of a vacuum. Second, Figure 6(b) shows the theoretical models of sliding TENG concept. In this model, top substrate is dielectric to dielectric layer and bottom substrate is metal to dielectric structure. The relation of voltage-transfer charges is expressed as :

$$V = -\frac{d_0}{W\varepsilon_0(l-x)}Q + \frac{\sigma d_0 x}{\varepsilon_0(l-x)} \quad (2)$$

Figure 6(c) shows the model of single electrode mode TENG. This model is consist of a dielectric layer and a metal electrode stacked face to face formation. Where, l is length, w is width, d_1 is thickness for dielectric 1, d_m is thickness of primary electrode. Figure 6(d) is the model of dielectric sliding mode TENG. Metal 1 and 2 are located in same layer with a gap g. This model's equation is expresed as :

$$dQ_1 = \frac{\sigma w dk}{1 + \frac{C_2(k)}{C_1(k)}} \quad (3)$$

$$dQ_2 = \frac{\sigma w dk}{1 + \frac{C_1(k)}{C_2(k)}} \quad (4)$$

A small area of dk is assumed to contain the tribo-charged density of σ, so total charge on the two electrode is σwdk.

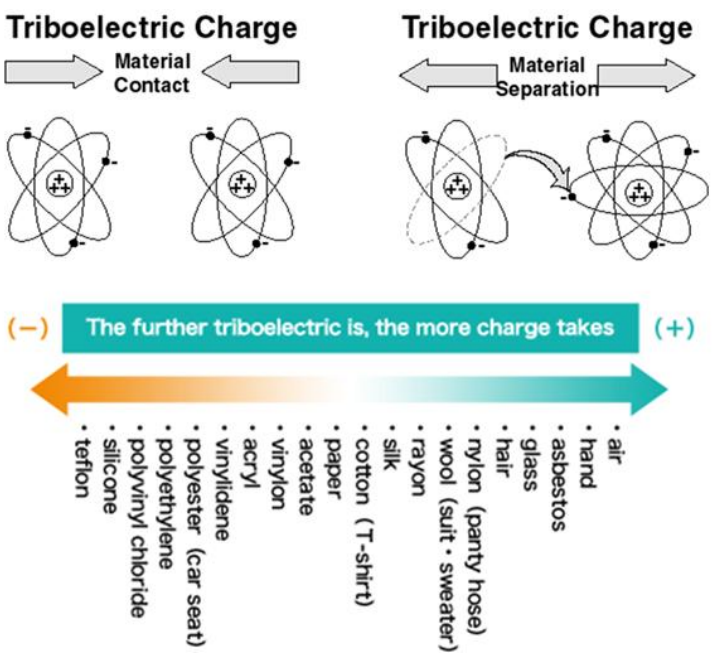

Figure 5. Triboelectric charge principle and triboelectric series.

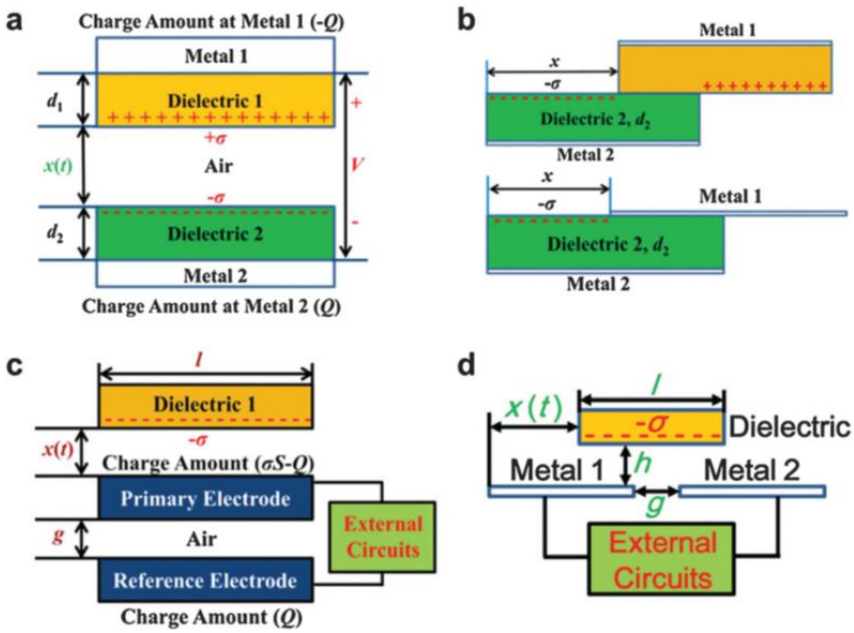

Figure 6. Fundamental theories of four working modes of TENGs. (a) The mode built for a dielectric-to-dielectric contact-mode TENG (b) The theoretical models of the dielectric-to-dielectric (up) and metal-to-dielectric (bottom) sliding mode TENG. (c) The theoretical models of the single electrode mode TENG. (d) The theoretical models of the sliding-mode freestanding TENG. (Reference 49)

Technologies trends for energy harvesting device

The beginning of TENG is the mode of vertical contact separation model.[53-55] Two different dielectric materials show inherent electrical properties of electron affinity when contact is happened. A voltage drop is generated by separating the two surface between upper and bottom electrodes. Two electrodes are connected with a resistor to flow the electron for balancing the electrostatic force. When the gap is close, the voltage drop is created by triboelectric. Then induced electrons flow according to the electric circuit. Electrical pulse of AC output is generated periodically. To improve the electrical output, various structure were designed of arch-shaped, spring-supported, zig-zag, and cantilever based.[56-59] The vertical contact-separation mode is useful to energy harvesting device from finger typing, engine vibration, human walking, biomedical systems. and self-powered sensors.[60-62]

Figure 7 (a) shows the contact with two opposite polarity materials polytetrafluoroethylene (PTFE) and aluminum causes the surface charge transfer.[63] This mode model is in-plane single mode. The surface electrons of aluminum move to the surface of PTFE because PTFE has a higher electron affinity than aluminum. This in-plane sliding mode have an advantage of high power output compare to vertical contact mode because its utilization of each surface is more effective than basic contact triboelectricity energy harvesting device. Furthermore, the in-plane sliding mode is easy to fabricate a more high performance structure owing to its simple structure.[64,65]

With constant sliding velocity is increase, the higher performance is achieved with same device. Single-electrode mode is for both the vertical contact-separation mode and in-plane sliding mode to jump the limitation of triboelectric nanogenerators. TENG is necessary to bond with electrode and electric wire. Figure 7 (c) shows the structure of single-electrode mode. But this mode has a shortage of low electrical power generation because its electrode is not effective to make surface rubbing.[66] So this mode TENG is suitable for various sensor consuming a few micro-watt. Free-standing triboelectric-layer mode is shown in Figure 7 (d). This mode can generate electricity using moving object. The freestanding triboelectric-layer mode has a small gap between the object and the electrode. The pressure of object bring the charge distribution from the electrode to another electrode. Asymmetric charge distribution cause the flow of electrons. This freestanding triboelectric-layer mode TENG has been applied for harvesting electrical energy with vibration, rotation motions.[67-69]

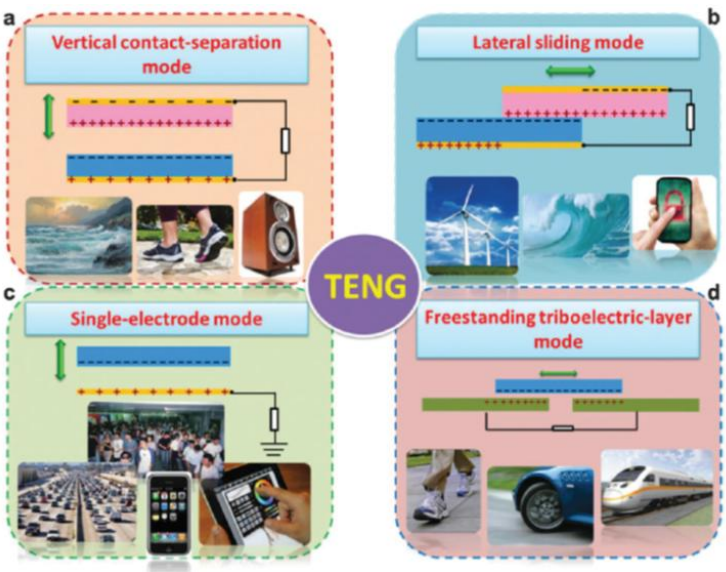

Figure 7. The four fundamental working modes of the triboelectric nanogenerators. (a) The vertical contact-separation mode. (b) The lateral sliding mode. (c) The single-electrode mode. (d) The free-standing mode. (Reference 63)

2.1.3 Thermoelectrics

Working Principle and application

Generally, physics of thermoelectricity are explained to the next three physical phenomena : the Seebeck effect, the Petier effect and the Thomson effect. Seebeck effect is the base of thermoelectric energy harvesting device. Temperature gradient of two different semiconductor materials connected in series generate open circuit voltage. Thermoelectric device is consist of two block : heat pumping and power generating. Heat pumping unit pumps heat from one side to the other side according to the direction of current flow. The power generation unit is related with energy conversion of heat flowing. The open-circuit thermoelectric potential Voc is expressed from the following equation :

$$V_{OC} = \alpha \Delta T \quad (1)$$

where ΔT[K] is the temperature difference of two junctions, and α [V/K] is the Seebeck coefficient, which gives the rate of change of Voc[v] with ΔT :

$$\alpha = \frac{\Delta V_{OC}}{\Delta T} \quad (2)$$

where, α is a coefficient with the materials and defined for ΔT is zero.

On the contrary to this, Peltier effect make a temperature gradient when specific voltage is applied two dissimilar materials. The Peltier effect was reported by the French physicist J.C.A. Peltier in 1844.

This phenomenon is the reversed Seebeck effect. The direction of current flow can control the heat absorption and dissipation in the form of heating and cooling. Peltier heating or cooling mean the variation with kinetic energy of a charge carrier.

The Peltier coefficient π is defined as :

$$\pi = \frac{P_P}{I} \qquad (3)$$

where P_p is the heat-transfer rate from the junction and I is the current flowing in the circuit. Finally, the Thomson effect was reported by Willian Thomson of British physicist. This phenomenon is about reversible absorption and emission of heat of a homogeneous materials exposed by thermal gradient. The current flows to the direction of high temperature when the conductor shows the increase of heat. The heat is expressed by :

$$P_T = \tau I \Delta T \qquad (4)$$

where, τ [V/K] is the Thomson coefficient. Thomson coefficient is for a single conductor but Seebeck and Peltier coefficient are for the junctions of two dissimilar conductor.

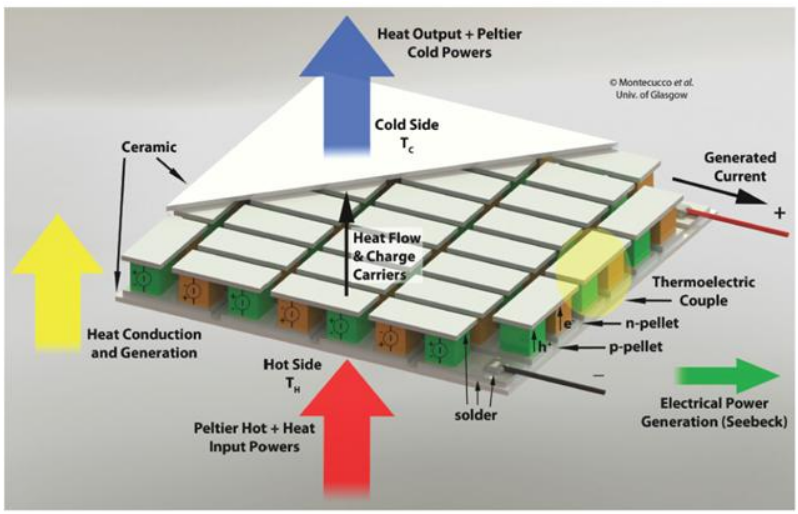

Figure 8. The concept of a thermoelectric generator showing the main physical effects.

Technologies trends for energy harvesting device

Doped semiconductors have a important role to improve the thermoelectric properties. Figure 8 shows the connection of p-type and n-type doped semiconductor of multiple pellets wired electrically in series and thermally in parallel. Each p-type and n-type doped semiconductor is called thermocouple. Thermocouple materials decide the voltage value of the thermoelectricity system.[70] Bismuth Telluride (Bi_2Te_3) is the most used material.[71-72] Modified Bismuth Telluride (Bi_2Te_3) thermocouple showed a Seebeck coefficient of 350 μV/K.[73] Large sized thermoelectric device consist of 127, 254 or 449 pair of thermocouples could generate open circuit voltage of 30V at ΔT.[74] Recently, the waste heat from the automotive is the hottest potential area of new approach of thermoelectricity. The temperature of exhaust gas from the engine or the pipe of the car has the range of 300-600 ℃ for diesel and 500-1000 ℃ for petrol. In 2001 Haidar's research team reported the application of medium and low temperature waste heat.[75] Anatychuck proposed thermoelectric generator system on diesel plant and achieved a maximum power produced of 1350W.[76] BMW of Germany was the first commercial car manufacturer to report a thermoelectric generator system and achieved 600W of electrical power for the on-vehicle test.[77] Risse and Zellbeck presented an interesting results from the thermal simulation of heat exchanger with a maximum of 358W.[78] In 1996, Bass and Killander reported a prototype thermoelectric generator for wood-red stoves with 10W from a 75 x 75 mm^2 TEG.[79] In 2004 Nuwayhid

reported a similar system producing up to 4.2W from a single 56 x 56 mm^2 TEG.[80] In 2010 Rinalde presented a prototype TEG system with red-wood stoves yielding 12.3 W from 200 ℃ with two TEGs.[81] In 2011 Champier presented a TEG system for stoves producing a maximum of 9.5W from a 56x56 mm^2.[82]

Bismuth Telluride (Bi2Te3) is the most used thermoelectricity generator material but its limitation of operating temperature is a maximum of 300 ℃. Silicides and Skutterudites materials are the candidate for the high temperature thermoelectricity generator in future.[83] Even though these material have a variety of issues, many scientist have investigated chemical reaction and electrical connection to overcome the temperature limitation.

Figure 9. Commercial car application for a thermoelectric generator system by BMW automotive.

2.2 Energy Harvesting Technologies Using Liquid

In 2011, Tom Kruenkin and J. Ashley Taylor research group of University of Wisconsin - Madison demonstrated new approach to high-power energy harvesting method using the flow of liquid metal. This new concept is called reverse electrowetting on dielectric (EWOD).[84] Reverse electrowetting is a contrary concept of electrowetting. The definition of electrowetting effect is explained as the conversion from mechanical to electrostatic force when an electrical potential is applied to liquid on dielectric layer.[85] The electrowetting phenomenon is understood in a view point of relationship wetting angle variation from the applied electrical force.[86] Additionally, electrowetting is a kind of thermodynamic phenomenon because of its surface tension is defined as the Gibbs free energy. The reverse electrowetting concept is derived from the motion of a conductive liquid on a dielectric. This is called electrowetting-on-dielectric (EWOD).[87]

In this paper, the change of wettability from the extra electrostatic force is related with charged liquid-solid interface, interfacial energy σ_{sl} is applied to Lippmann's effective solid-liquid interfacial energy :

$$\sigma_{sleff} = \sigma_{sl} - CV^2/2 \qquad (1)$$

where V is the voltage between the conductive droplet and the dielectric layer and C is the capacitance per unit area. This equation is also expressed in terms of contact angle θ,

$$\cos\theta = \cos\theta_0 + CV^2/2\sigma_{lv} \qquad (2)$$

where σ_{iv} is the interfacial energy of the liquid-vapor and θ_0 is the contact angle of initial droplet. In the beginning of this experiment, oscillating plate type energy harvesting device is introduced shown in Figure 9. This plate is consist of upper and bottom substrate with dielectric layer on conductive film. They demonstrated this device using single conductive liquid drop to 150 droplets.[88] Conductive Galinstan and Mercury droplets were introduced for generating electrical output. Resulting power density showed 10^{-1} W cm^{-2} at 50 Hz frequency with vibration type while the major other experimental results showed output power from 10^{-6} to 10^{-2} W. Zhaochu Yang, Einar Halvorsen and Tao Dong research group expressed power generation results using conductive droplet sliding on electret film using liquid Mucury.[89] Conventional electrostatic energy harvesting device need the external voltage supply to fix the surface charge polarization negatively or positively.[90] In this study, a thin polytetrafluoroethylene (PTFE) electret is employed for core material generating variable capacitance. The sliding of conductive Mucury droplet on PTFE in the patterned electrode generated 0.18 μW with 1.2mm diameter without any external electrical source. Electrical double layer (EDL) phenomenon is the new source of the energy harvesting device using liquid.[91] The model of EDL was proposed by Helmholtz in 1850. EDL is a layer of object exposed in a fluid. If a solid particle is contact with liquid, there are two parallel layer is formed. EDL refers to the parallel layer surrounding the particle. The surface charge of the first layer attract the ions owing to the

chemical interactions. The second layer is consist of ions adsorbed on the first surface. The bonding force of the second layer is weak because of screening force of the first layer. This results make the free ions that move in the fluid and we call it diffuse layer.[92] The charges of two layers (double layer) by the adsorbed ions cause the potential drop in the solution shown in Figure 10. In 2012, Jong Kyun Moon, Jaeki Jeong1, Dongyun Lee & Hyuk Kyu Pak research group proposed a new method of AC electrical power generation by using plain water, without the need for any external bias-voltage source.[93] In this paper, the water plays a role of transferring charge of ions. The research team found that AC electric current is generated by a mechanical modulation in the water bridge between upper substrate and bottom substrate even though the maximum size of water bridge is restricted by the capillary length of water droplet. This limitation is solved by introduction of numerous water droplet on dielectric layer. In this results, the maximum power density is 0.3 μWcm^{-2} using 1 ml of water. In 2014, Jun Yin et al demonstrated graphene/liquid systems for energy harvesting device.[94] In this paper , electrokinetic phenomena occurred because an electrical double layer created the interface of ionic liquids and graphene. A few millivolts of electrical power is induced by the moving of a droplet of ionic fluid on the graphene substrate. Final prototype of an energy harvesting device showed a pulse type voltage of about 30 mV using a droplet of 80 μl 0.6 M $CuCl_2$ solution. The drawing of the droplet from 15 cm onto a 70 degree tilted graphene surface realized the generation of

electrical power. Moving of ionic liquid droplet can generate the electricity owing to an electrokinetic phenomenon related with pseudocapacitor effect.[95] This operation principle helps to the various application such as velocity sensor, a handwriting sensor and energy harvesting device. Kim's research team discussed the relationship of the interface between solid surface and ionic liquid.[96] When an ionic liquid is contact with a polymer material surface, an electrical double layer is formed by its attraction property. In this paper, the electrical output is 5 μW of 3 V using 80 μL water of 0.01 M NaCl droplet. This active transducer without external electrical source is consist with poly4-vinylphenol (P4VP) layer and silica gel film made by sol-gel process. EDL is the core factor to affect the driving of ion dynamic from the results. Fluidic electricity generator is also the representative example for energy harvesting device using EDL. In 2015, Y.J. Yang reported that two phase of water flow and air flow could generate the electricity by modulating EDL. The structure of this device is the type of tube.[97] They verified this device detects air bubble in the water flow without any external electrical input. The average peak power was 5.64 nW using 10 cm length water flow and 30 cm air sequence with a flow rate of 30 ml/min.

The various liquids including water are also related with triboelectric energy harvesting device. In 2016, S.S Kwak et al reported the possibility of large electric power generation from a single moving water droplet on a mono-layer graphene.[98] In this experiment, they found the new method producing an output power of 1.9 μW, 100

times larger than their past results.[99] The mono-layer graphene on polytetrafluoroethylene (PTFE) is the important reason inducing the triboelectrification with pseudocapacitance between a water droplet and the monolayer graphene. TENG above mentioned, is also the promising candidate of energy harvesting method using water. A patterned polydimethylsiloxane (PDMS) provided an high open circuit voltage of 52 V and a short circuit current of 2.45 mA^{-2} with a peak power density of 0.13 Wm^{-2}. This TENG using water are designed for the contact of water and solid materials compare to conventional TENG device.[100]

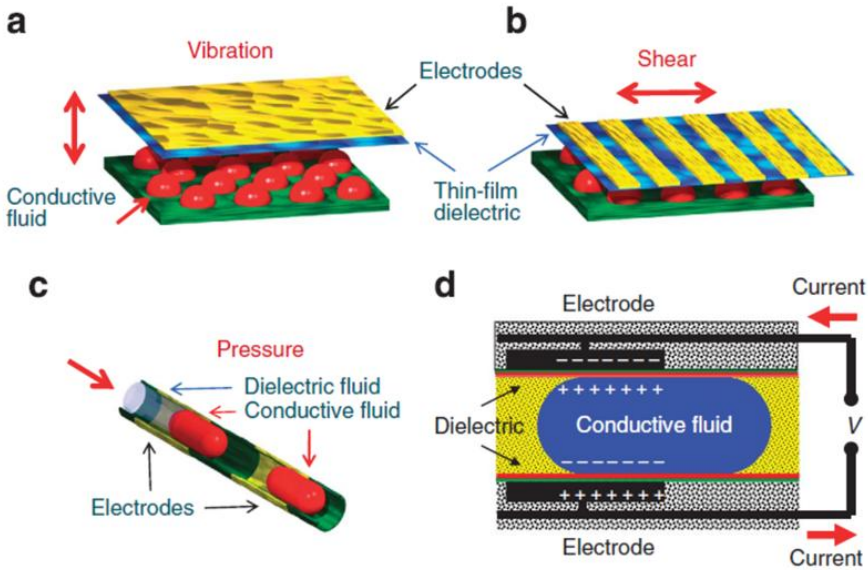

Figure 9. Schematics of three major droplet actuation mechanisms. These include (a) droplets between oscillating plates, (b) droplets between sliding plates, and (c) droplets in a micro-channel. (d) Shows in greater detail schematics of reverse-electrowetting-based energy generation process in a micro-channel geometry. (Reference 88)

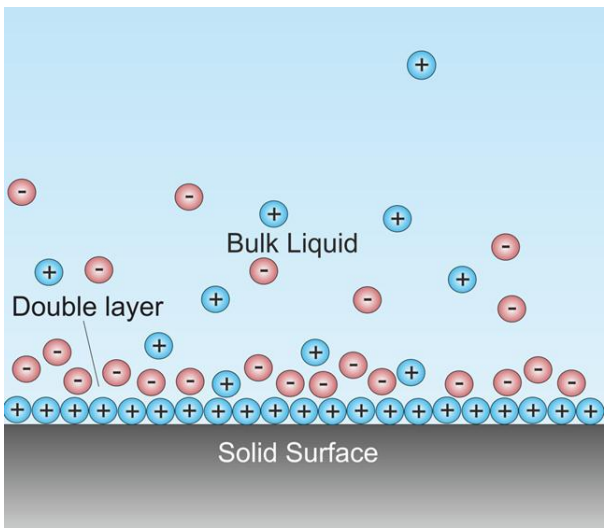

Figure 10. Schematic of double layer in a liquid at contact with a negatively-charged solid. Depending on the nature of the solids, there may be another double layer (unmarked on the drawing) inside the solid.

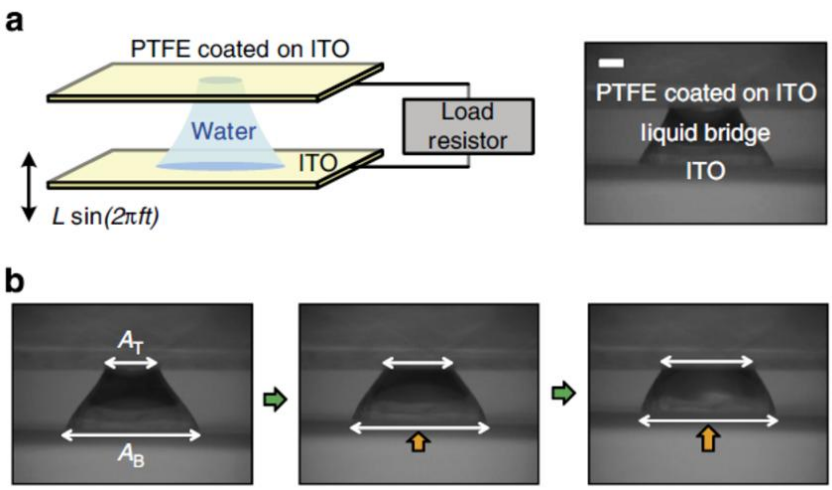

Figure 11. Schematic diagram of the experiment and resistor-capacitor circuit model. (a) Experimental setup and (b) video images of water bridge over time. Scale bar, 1 mm. (Reference 93)

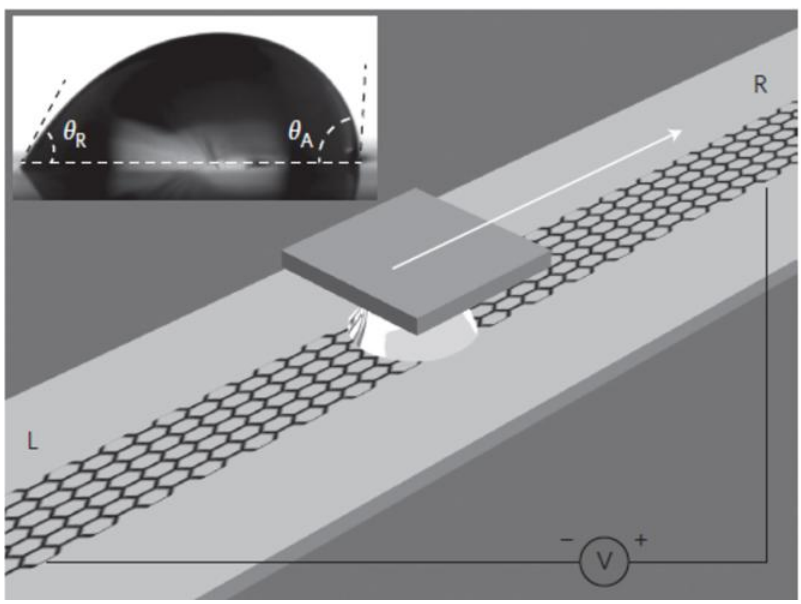

Figure 12. A liquid droplet is sandwiched between graphene and a SiO2/Si wafer, and drawn by the wafer at specific velocities. Inset: a droplet of 0.6 M NaCl solution on a graphene surface. (Reference 94)

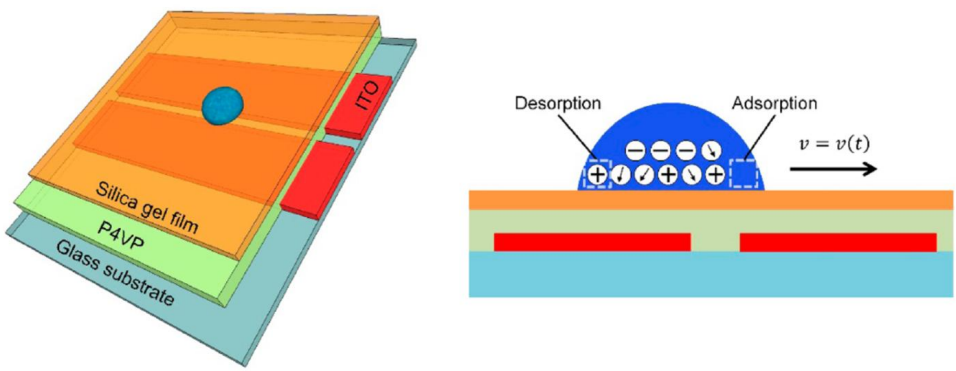

Figure 13. Schematic image of the active transducer and The schematic cross-sectional image of the active transducer in the dynamic state. Cations, anions, and the water molecule (depicted by a circle surrounding an arrow) formed the electrical double layer (EDL). (Reference 97)

2.3 References

1 Beeby, S. P, M. J Tudor, and N. M. White, "Energy harvesting vibration sources for microsystems applications", Meas Sci Technol, 17(12), 2006, R175.

2 Ottman, G. K, Hofmann, H. F, Bhatt, A. C, & Lesieutre, G. A, "Adaptive piezoelectric energy harvesting circuit for wireless remote power supply", IEEE Transactions on power electronics, 17(5), 2002, 669-676.

3 Tutuncuoglu, Kaya, and Aylin Yener, "Optimum transmission policies for battery limited energy harvesting nodes" IEEE Transactions on Wireless Communications, 11(3), 2012, 1180-1189.

4 Priya, Shashank, and Daniel J. Inman, "Energy harvesting technologies", Vol(21), New York : Springer, 2009.

5 Chalasani, Sravanthi, and James M. Conrad, "A survey of energy harvesting sources for embedded systems" IEEE SoutheastCon, 2008.

6 Harb, Adnan, "Energy harvesting : State-of-the-art" Renewable Energy, 36(10), 2011, 2641-2654.

7 Challa, V. R, Prasad, M. G, Shi, Y, & Fisher, F. T, "A vibration energy harvesting device with bidirectional resonance frequency tunability", Smart Mater Struct, 17(1), 2008, 015035.

8 S.P. Beeby, M.J. Tudor, N.M, "White Energy harvesting vibration sources for microsystems applications Meas", Sci. Technol, 17, 2006, 175 - 195.

9 W.J. Li, T.C.H. Ho, G.M.H. Chan, P.H.W. Leong, H.Y. Wong, "Infrared signal transmission by a laser-micromachined vibrationinduced power generator", Proceedings of the 43rd IEEE Midwest Symposium on Circuits and Systems, vol(1), 2000, 236 - 239.

10 Guyomar, D, Sebald, D, Pruvost, S, Lallart, M, Khodayari, A, & Richard, C, "Energy harvesting from ambient vibrations and heat", J Intell Mater Syst Struct, 2008.

11 Chiba, S, Waki, M, Kornbluh, R, & Pelrine, R, "Innovative power generators for energy harvesting using electroactive polymer artificial muscles", The 15th International Symposium on : Smart Structures and Materials & Nondestructive Evaluation and Health Monitoring, International Society for Optics and Photonics, 2008.

12 K. Uchida, S. Takahashi, K. Harii, J. Ieda, W. Koshibae, K. Ando1, S. Maekawa & E. Saitoh, "Observation of the spin Seebeck effect", Nature, 2008, 778-781.

13 Boyer, A, and E. Cisse, "Properties of thin film thermoelectric materials: application to sensors using the Seebeck effect", Mater Sci Eng B, 13(2), 1992, 103-111.

14 Astrain, D, J. G. Vián, and J. Albizua, "Computational model for refrigerators based on Peltier effect application", Appl Therm Eng, 25(17), 2005, 3149-3162.

15 Erturk, Alper, and Daniel J. Inman, "Piezoelectric energy harvesting", John Wiley & Sons, 2011.

16 Cook-Chennault, K. A, N. Thambi, and A. M. Sastry, "Powering MEMS portable devices－a review of non-regenerative and regenerative power supply systems with special emphasis on piezoelectric energy harvesting systems", Smart Mater Struct, 17(4), 2008, 043001.

17 Nomura, Toshiyuki, Takeshi Satoh, and Hiroaki Masuda, "The environment humidity effect on the tribo-charge of powder", Powder Technology, 135, 2003, 43-49.

18 Sodano, Henry A, Daniel J. Inman, and Gyuhae Park, "Comparison of piezoelectric energy harvesting devices for recharging batteries", J Intell Mater Syst Struct, 2005, 799-807.

19 Gururaja, T. R, Schulze, W. A, Cross, L. E, Newnham, R. E, Auld, B. A, & Wang, Y. J, "Piezoelectric composite materials for ultrasonic transducer applications. Part I: Resonant modes of vibration of PZT rod-polymer composites", IEEE Trans. Sonics Ultrason, 1985, 481-498.

20 Furukawa, Takeo, Koji Fujino, and Eiichi Fukada, "Electromechanical properties in the composites of epoxy resin and PZT ceramics", Jpn J Appl Phys, 15(11), 1976, 2119.

21 Kim, K.B, Kim, C.I, Jeong, Y.H, Lee, Y.J, Cho, J.H, Paik, J.H, Nahm, S, "Performance of unimorph cantilever generator using Cr/Nb doped $Pb(Zr0.54Ti0.46)O_3$ thick film for energy harvesting device applications", J. Eur.Ceram. Soc, 33, 2013, 305 - 311.

22 Choi, C.H, Seo, I.T, Song, D, Jang, M.S, Kim, B.Y, Nahm, S, Sung, T.H, Song, H.C, "Relation between piezoelectric properties of ceramics and output power density of energy harvester" J. Eur. Ceram. Soc, 33, 2013, 1343 - 1347.

23 Kim, S.B, Park, J.H, Ahn, H, Liu, D, Kim, D.J, "Temperature effects on output power of piezoelectric vibration energy harvesters", Microelectron. J, 42, 2011, 988 - 991.

24 Song, H.C, Kang, C.Y, Yoon, S.J, Jeong, D.Y, "Engineered domain configuration and piezoelectric energy harvesting in $0.7Pb(Mg1/3Nb2/3)O_3 - 0.3PbTiO_3$ single crystals", Metals Mater. Int, 18, 2012, 499 - 503.

25 Berdy, D.F, Srisungsitthisunti, P, Jung, B, Xu, X.F, Rhoads, J.F, Peroulis, D "Low-frequency meandering piezoelectric vibration energy harvester", IEEE Trans. Ultrason. Ferroelectr. Freq. Control, 59, 2012, 846 - 858.

26 Shindo, Y, Narita, F, "Dynamic bending/torsion and output power of s-shaped piezoelectric energy harvesters", Int. J. Mech. Mater. Des, 10, 2014, 305 - 311.

27 Sobocinski, M, Leinonen, M, Juuti, J, Jantunen, H, "Monomorph piezoelectric wideband energy harvester integrated into LTCC", J. Eur. Ceram. Soc, 31, 2011, 789 - 794.

28 Palosaari, J, Leinonen, M, Hannu, J, Juuti, J, Jantunen, H, "Energy harvesting with a cymbal type piezoelectric transducer from low frequency compression", J. Electroceram, 28, 2012, 214 - 219.

29 Chen, X.R, Yang, T.Q, Wang, W, Yao, X, "Vibration energy harvesting with a clamped piezoelectric circular diaphragm", Ceram. Int, 38, 2012, 271 - S274.

30 Makki, N, Pop-Iliev, R, "Battery- and wire-less tire pressure measurement systems (TPMS) sensor", Microsyst.Technol, 18, 2012, 1201-1212.

31 Janphuang, P, Lockhart, R, Uffer, N, Briand, D, de Rooij, N.F, "Vibrational piezoelectric energy harvesters based on thinned bulk PZT sheets fabricated at the wafer level", Sens. Actuators A Phys, 210, 2014, 1 - 9.

32 Cui, Y, Zhang, Q.Y, Yao, M.L, Dong, W.J, Gao, S.Q, "Vibration piezoelectric energy harvester with multi-beam", AIP Adv, 5, 2015, 041332.

33 Deng, L.C, Wen, Z.Y, Zhao, X.Q, Yuan, C.W, Luo, G.X, Mo, J.K, "High voltage output MEMS vibration energy harvester in d31 mode with PZT thin film", J. Microelectromech. Syst, 23, 2014, 855 - 861.

34 Liu, H.C, Zhang, S.S, Kobayashi, T, Chen, T, Lee, C, "Flow sensing and energy harvesting characteristics of a wind-driven piezoelectric Pb(Zr0.52, Ti0.48)O_3 microcantilever", Micro Nano Lett, 9, 2014, 286 - 289.

35 Kim, M, Hwang, B, Min, N.K, Jeong, J, Kwon, K.H, Park, K.B, "Design and fabrication of a PZT cantilever for low frequency vibration energy harvesting", J. Nanosci. Nanotechnol, 11, 2011, 6510 - 6513.

36 Kim, M, Hwang, B, Jeong, J, Min, N.K, Kwon, K.H, "Micromachining of a bimorph $Pb(Zr,Ti)O_3$ (PZT) cantilever using a micro-electromechanical systems (MEMS) process for energy harvesting application", J. Nanosci. Nanotechnol, 12, 2012, 6011 - 6015.

37 Kim, S.B, Park, H, Kim, S.H, Wikle, H.C, Park, J.H, Kim, D.J, "Comparison of MEMS PZT cantilevers based on d(31) and d(33) modes for vibration energy harvesting", J. Microelectromech. Syst, 22, 2013, 26 - 33.

38 Tang, G, Liu, J.Q, Yang, B, Luo, J.B, Liu, H.S, Li, Y.G, Yang, C.S, He, D.N, Dao, V.D, Tanaka, K, "Fabrication and analysis of high-performance piezoelectric MEMS generators", J. Micromech. Microeng, 22, 2012, 065017.

39 Tang, G, Liu, J.Q, Liu, H.S, Li, Y.G, Yang, C.S, He, D.N, DzungDao, V, Tanaka, K, Sugiyama, S, "Piezoelectric MEMS generator based on the bulk PZT/silicon wafer bonding technique", Phys. Status Solidi A, 208, 2011, 2913 - 2919.

40 Kuehne, I, Schreiter, M, Seidel, J, Seidel, H, Frey, A, "A novel MEMS design of a piezoelectric generator for fluid-actuated energy conversion", Proc. SPIE 2011, 8066, 806617.

41 Lin, S.C, Wu, W.J, "Piezoelectric micro energy harvesters based on stainless-steel substrates", Smart Mater.Struct, 22, 2013, 045016.

42 Liu, H.C, Tay, C.J, Quan, C.G, Kobayashi, T, Lee, C,

"Piezoelectric MEMS energy harvester for low-frequency vibrations with wideband operation range and steadily increased output power", J. icroelectromech. Syst, 20, 2011, 1131 - 1142.

43 Liu, H.C, Quan, C.G, Tay, C.J, Kobayashi, T, Lee, C, "A MEMS-based piezoelectric cantilever patterned with PZT thin film array for harvesting energy from low frequency vibrations", Phys. Proc, 19, 2011, 129 - 133.

44 Ambrose, J. R, and J. Kruger, "Tribo-ellipsometry : A new technique to study the relationship of repassivation kinetics to stress corrosion", Corrosion, 28(1), 1972, 30-35.

45 Nomura, Toshiyuki, Takeshi Satoh, and Hiroaki Masuda, "The environment humidity effect on the tribo-charge of powder", Powder Technology, 135, 2003, 43-49.

46 Shaw, P. E, "Experiments on tribo-electricity. I. The tribo-electric series", Proceedings of the Royal Society of London. Series A, Containing Papers of a Mathematical and Physical Character, 1917, 16-33.

47 Deli, Gong, Xue Qunji, and Wang Hongli, "ESCA study on tribochemical characteristics of filled PTFE", Wear, 148(1), 1991, 161-169.

48 Martin, Jean Michel, "Antiwear mechanisms of zinc dithiophosphate: a chemical hardness approach", Tribology letters, 6(1), 1999, 1-8.

49 Wang, Zhong Lin, Jun Chen, and Long Lin, "Progress in

riboelectric nanogenerators as a new energy technology and self-powered sensors", Energy Environ Sci, 8(8), 2015, 2250-2282.

50 Wang, Sihong, "Freestanding Triboelectric Layer Based Nanogenerators for Harvesting Energy from a Moving Object or Human Motion in Contact and Non contact Modes", Adv Mater, 26(18), 2014, 2818-2824.

51 Yang, Ya, "Triboelectric nanogenerator for harvesting wind energy and as self-powered wind vector sensor system", ACS nano, 7(10), 2013, 9461-9468.

52 Zhu, Guang, et al, "Power-generating shoe insole based on triboelectric nanogenerators for self-powered consumer electronics", Nano Energy, 2(5), 2013, 688-692.

53 Zhu, G, Pan, C, Guo, W, Chen, C. Y, Zhou, Y, Yu, R, & Wang, Z. L, "Triboelectric-generator-driven pulse electrodeposition for micropatterning", Nano Lett, 12(9), 2012, 4960-4965.

54 Wang, Sihong, Long Lin, and Zhong Lin Wang, "Nanoscale triboelectric-effect-enabled energy conversion for sustainably powering portable electronics", Nano Lett, 12(12), 2012, 6339-6346.

55 Fan, F. R, Lin, L, Zhu, G, Wu, W, Zhang, R, & Wang, Z. L, "Transparent triboelectric nanogenerators and self-powered pressure sensors based on micropatterned plastic films", Nano Lett, 12(6), 2012, 3109-3114.

56 G. Zhu, Z.-H. Lin, Q. Jing, P. Bai, C. Pan, Y. Yang, Y. Zhouand Z. L. Wang, "Toward large-scale energy harvesting by a nanoparticle-enhanced triboelectric nanogenerator" Nano Lett, 13(2), 2013, 847-853.

57 J. Chen, G. Zhu, W. Yang, Q. Jing, P. Bai, Y. Yang, T.-C. Houand Z. L. Wang, "Harmonic resonator based triboelectric nanogenerator as a sustainable power source and a self powered active vibration sensor", Adv Mater, 25(42), 2013, 6094-6099.

58 P. Bai, G. Zhu, Z.-H. Lin, Q. Jing, J. Chen, G. Zhang, J. Ma and Z. L. Wang, "Integrated multilayered triboelectric nanogenerator for harvesting biomechanical energy from human motions" ACS nano, 7(4), 2013, 3713-3719.

59 G. Zhu, P. Bai, J. Chen and Z. L. Wang, "Power-generating shoe insole based on triboelectric nanogenerators for self-powered consumer electronics", Nano Energy, 2(5), 2013, 688-692.

60 J. Zhong, Q. Zhong, F. Fan, Y. Zhang, S. Wang, B. Hu,Z. L. Wang and J. Zhou, "Finger typing driven triboelectric nanogenerator and its use for instantaneously lighting up LEDs", Nano Energy, 2(4), 2013, 491-497.

61 W. Yang, J. Chen, G. Zhu, J. Yang, P. Bai, Y. Su, Q. Jing,X. Cao and Z. L. Wang, "Harvesting energy from the natural vibration of human walking", ACS nano, 7(12), 2013, 11317-11324.

62 T.-C. Hou, Y. Yang, H. Zhang, J. Chen, L.-J. Chen andZ. L. Wang, "Triboelectric nanogenerator built inside shoe insole for harvesting walking energy", Nano Energy, 2(5), 2013, 856-862.

63 Wang, Zhong Lin, "Triboelectric nanogenerators as new energy technology and self-powered sensors - Principles, problems and perspectives", Faraday Discuss, 176, 2014, 447-458.

64 G. Zhu, J. Chen, Y. Liu, P. Bai, Y. S. Zhou, Q. Jing, C. Panand Z. L. Wang, "Linear-grating triboelectric generator based on sliding electrification", Nano Lett, 13(5), 2013, 2282-2289.

65 G. Zhu, J. Chen, T. Zhang, Q. Jing and Z. L. Wang, "Radial-arrayed rotary electrification for high performance triboelectric generator", Nat Commun, 5, 2014.

66 S. Niu, Y. Liu, S. Wang, L. Lin, Y. S. Zhou, Y. Hu andZ. L. Wang, "Theoretical Investigation and Structural Optimization of Single Electrode Triboelectric Nanogenerators", Adv Funct Mater, 24(22), 2014, 3332-3340.

67 S. Wang, S. Niu, J. Yang, L. Lin and Z. L. Wang, "Quantitative measurements of vibration amplitude using a contact-mode freestanding triboelectric nanogenerator", ACS nano, 8(12), 2014, 12004-12013.

68 H. Guo, J. Chen, M.-H. Yeh, X. Fan, Z. Wen, Z. Li, C. Huand Z. L. Wang, "An ultrarobust high-performance triboelectric nanogenerator based on charge replenishment", ACS nano,

9(5), 2015, 5577-5584.

69 L. Lin, S. Wang, S. Niu, C. Liu, Y. Xie and Z. L. Wang, "Noncontact free-rotating disk triboelectric nanogenerator as a ustainable energy harvester and self-powered mechanical sensor", ACS Appl Mater Interfaces, 6(4), 2014, 3031-3038.

70 Tritt, Terry M, and M. A. Subramanian, "Thermoelectric materials, phenomena, and applications: a bird's eye view", MRS bulletin, 31(03), 2006, 188-198.

71 Tang, X, Xie, W, Li, H, Zhao, W, Zhang, Q, & Niino, M, "Preparation and thermoelectric transport properties of high-performance p-type Bi2Te3 with layered nanostructure", Appl Phys Lett, 90(1), 2007, 12102-12102.

72 You, H, Bae, S. H, Kim, J, Kim, J. S, & Park, C, "Deposition of nanocrystalline Bi_2Te_3 films using a modified MOCVD system", J ELECTRON MATER, 40(5), 2011, 635-640.

73 Goldsmid, H. Julian, "Bismuth telluride and its alloys as materials for thermoelectric generation", Materials, 7(4), 2014, 2577-2592.

74 Montecucco, Andrea, Jonathan Siviter, and Andrew R. Knox, "The effect of temperature mismatch on thermoelectric generators electrically connected in series and parallel", Appl Energy, 123, 2014, 47-54.

75 Haidar, Jihad G, and Jamil I. Ghojel, "Waste heat recovery from the exhaust of low-power diesel engine using thermoelectric generators", Thermoelectrics, 2001.

76 L. I. Anatychuk, R. V. Kuz, and Y. Y. Rozver, "Efficiency of thermoelectric recuperators of the exhaust gas energy of internal combustion engines", 9TH EUROPEAN CONFERENCE ON THERMOELECTRICS: ECT2011. Vol. 1449. No. 1. AIP Publishing, 2012.

77 D. Crane, J. LaGrandeur, V. Jovovic, M. Ranalli, M. Adldinger, E. Poliquin, J. Dean, D. Kos-sakovski, B. Mazar, and C. Maranville, "TEG on-vehicle performance and model validation and what it means for further TEG development", J ELECTRON MATER, 42(7), 2013, 1582-1591.

78 Risse, Ing Silvio, and Ing Hans Zellbeck, "Close-coupled exhaust gas energy recovery in a gasoline engine", MTZ worldwide, 74(1), 2013, 54-61.

79 Killander, Anders, and John C. Bass, "A stove-top generator for cold areas", Thermoelectrics, 1996, Fifteenth International Conference on. IEEE.

80 Shihadeh, A, R. Nuwayhid, and N. Ghaddar, "Development and testing of a domestic woodstove thermoelectric generator with natural convection cooling", Energy Convers Manag, 2004.

81 G. Rinalde, L. Juanico, E. Taglialavore, S. Gortari, and M. Molina, "Development of thermoelectric generators for electrification of isolated rural homes", Int J Hydrogen Energy, 35(11), 2010, 5818-5822.

82 D. Champier, J. P. Bedecarrats, T. Kousksou, M. Rivaletto, F. Strub, and P. Pignolet, "Study of a TE (thermoelectric)

generator incorporated in a multifunction wood stove", Energy 36(3), 2011, 1518-1526.

83 Fergus, Jeffrey W, "Oxide materials for high temperature thermoelectric energy conversion", J Eur Ceram Soc, 32(3), 2012, 525-540.

84 Mugele, Frieder, Michel Duits, and Dirk Van den Ende, "Electrowetting: a versatile tool for drop manipulation, generation, and characterization", Adv Colloid Interface Sci, 161(1), 2010, 115-123.

85 Lin, Y. Y, Evans, R. D, Welch, E, Hsu, B. N, Madison, A. C, & Fair, R. B. l, "Low voltage electrowetting-on-dielectric platform using multi-layer insulators", Sens Actuators B Chem, 150(1), 2010, 465-470.

86 Quilliet, Catherine, and Bruno Berge, "Electrowetting: a recent outbreak", Curr Opin Colloid Interface Sci, 6(1), 2001, 34-39.

87 Gong, Jian, "All-electronic droplet generation on-chip with real-time feedback control for EWOD digital microfluidics", Lab Chip, 8(6), 2008, 898-906.

88 Krupenkin, Tom, and J. Ashley Taylor, "Reverse electrowetting as a new approach to high-power energy harvesting", Nat Commun, 2, 2011, 448.

89 Yang, Zhaochu, Einar Halvorsen, and Tao Dong, "Power generation from conductive droplet sliding on electret film", Appl Phys Lett, 100(21), 2012, 213905.

90 Sessler, Gerhard M, "Electrets: recent developments", J

Electrostat, 51, 2001, 137-145.

91 Yates, David E, Samuel Levine, and Thomas W. Healy, "Site-binding model of the electrical double layer at the oxide/water interface", J. Chem. Soc., Faraday Trans. 1, 70, 1974, 1807-1818.

92 Delahay, Paul, "Double layer and electrode kinetics", John Wiley & Sons Inc, 1965.

93 Moon, J. K, Jeong, J, Lee, D, & Pak, H. K, "Electrical power generation by mechanically modulating electrical double layers", Nat Commun, 4, 2013, 1487.

94 Jun Yin, Xuemei Li, Jin Yu, Zhuhua Zhang, Jianxin Zhou and Wanlin Guo, "Generating electricity by moving a droplet of ionic liquid along graphene", Nat Nanotechnol, 9(5), 2014, 378-383.

95 Lyklema, Hans, "General preface", Fundamentals of Interface and Colloid Science 2, Elsevier, 1995, 5-6.

96 Junwoo Park,YoungJun Yang, Soon-Hyung Kwon and Youn Sang Kim, "Influences of surface and ionic properties on electricity generation of an active transducer driven by water motion", J Phys Chem Lett, 6(4), 2015, 745-749.

97 YoungJun Yang, Junwoo Park, Soon-Hyung Kwon and Youn Sang Kim, "Fluidic Active Transducer for Electricity Generation", Sci. Rep, 5, 2015.

98 Sung Soo Kwak, Shisheng Lin, Jeong Hwan Lee, Hanjun Ryu, Tae Yun Kim, Huikai Zhong, Hongsheng Chen, and

Sang-Woo Kim, "Triboelectrification-Induced Large Electric Power Generation from a Single Moving Droplet on Graphene/Polytetrafluoroethylene", ACS nano, 10(8), 2016, 7297-7302.

99 Yin, J, Zhang, Z, Li, X, Yu, J, Zhou, J, Chen, Y, & Guo, W, "Waving potential in graphene", Nat Commun, 5, 2014.

100 Zong-Hong Lin, Gang Cheng, Long Lin, Sangmin Lee, and Zhong Lin Wang, "Water - Solid Surface Contact Electrification and its Use for Harvesting Liquid Wave Energy", Angew Chem Int Ed Engl, 52(48), 2013, 12545-12549.

Chapter 3. Water Motion Active Transducer

3.1 Overview & Motivation

Dielectric materials, including polymers, show a permanent polarization characteristic owing to their asymmetrical molecular structure.[1,2] When the surface of dielectric materials make contact with water, although the water molecules are electrically neutral, a thin electric double layer (EDL) is formed at the interface.[3] The electrostatic charges on the surface attract the counter ions of water droplets.[4-6] Both the surface polarity of the dielectric materials and the EDL carry electric charges. This phenomenon, related to an EDL, can be explored as an energy conversion method. Many research groups have demonstrated the use of the EDL for energy conversion through electro-osmosis, electrophoresis, and streaming currents.[7-9] In recent years, impressive EDL experimental results for energy harvesting between water and solid state have been achieved.[10,11] The electrical power generation method, which mechanically modulates the EDL, successfully generated electricity without any electromagnetic induction.8 Additionally, the contact electrical cation between the water and polydimethylsiloxane (PDMS) showed that the EDL system is capable of converting mechanical energy into electricity.[12] Despite the remarkable progress in their research, these energy conversion devices have a drawback as they need an initial kinetic energy source, such as artificial intermittent stimulation by pressing, bending,

vibration or friction.[12-16] These external forces required for energy harvesting are not natural phenomena occurring in our surroundings, such as raindrops or ocean waves. Moreover, they need complex manufacturing processes, for example, nano-wires, micro-patterned layers, or multi-layered processes, which have high manufacturing costs.[17-19] Lately scientists and engineers are developing new technologies to harvest waste energy using thermoelectricity, piezoelectricity or reverse electrowetting but they are struggling with low energy conversion efficiency and low electric power generation of these devices.[20-22] These devices need specific structure and condition to generate the electrical energy. Some methods need toxic chemical materials for charge transferring medium. So these devices have the limitation of power generation scale compare to the hydropower generator which generate the electricity from constant and abundant energy source as mentioned. To overcome these limitations, herein we propose a new active transducer for the effective generation of electric power from the natural motion of water without any external sources or processes. A water motion active transducer (WMAT) was designed with a simple structure, and an effective process was established using a solution process for low-cost production. A water droplet which was in contact with a poly-4-vinyl phenol (PVP) dielectric material was positively charged due to the negative polarity of the polymer layer. We observed that variation of the overlapping area between the water and dielectric layer could effectively induce electric charge through the electrode under the dielectric layer. Using

the motion of a 30 mL droplet of tap-water, we could successfully generate electricity with a peak voltage of 3.1 V and peak current of 5.3 mA, which was enough to turn on a green LED.

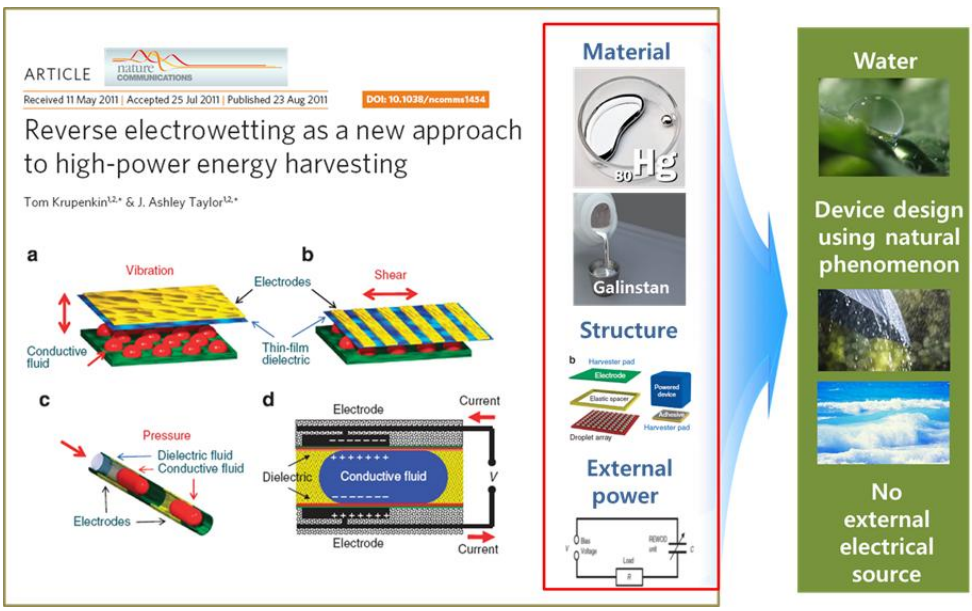

Figure 14. The limitation of conventional energy harvesting device and the motivation of WMAT experiment.

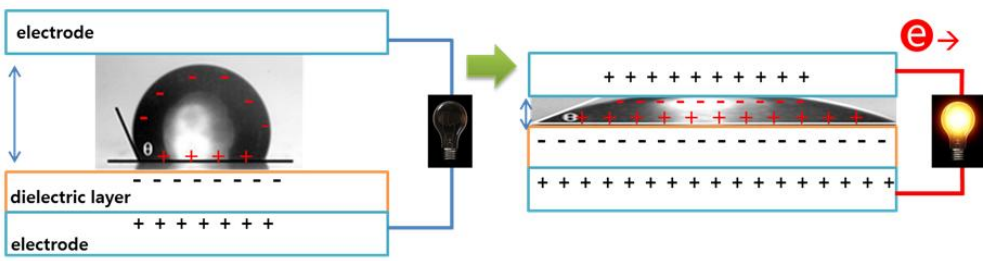

Figure 15. Fundamental operation principle water motion active transducer (WMAT) using electrical double layer (EDL)

3.2 Water Motion Active Transducer Structure & Material

The WMAT was composed of pre-patterned ITO as an electrode, PVP as a dielectric layer, and EKG-6015N (ETC Company, Germany) as a hydrophobic layer (Figure 16). The electrodes were laid on the glass perpendicularly with respect to the flowing direction of the water droplet. PVP layer was spin-coated on the patterned ITO glass substrate. Then, hydrophobic layer, EKG-6015N solution was coated on PVP layer. Detail fabrication was introduced in experimental section. WMAT was transparent because of transparent electrodes, very thin dielectric and hydrophobic layers shown in Figure 16. Scanning electron microscopy (SEM) was conducted to observe the thickness of WMAT, respectively. The thickness of PVP layer was 290 nm and that of ITO electrode layer was 120 nm. Considering the size of natural water droplet such as raindrop, width and gap of electrode was designed with 7 mm and 2 mm. For smooth sliding of water droplets, the hydrophobic layer, EKG-6015N, was adopted on the PVP dielectric layer shown in Figure 18.

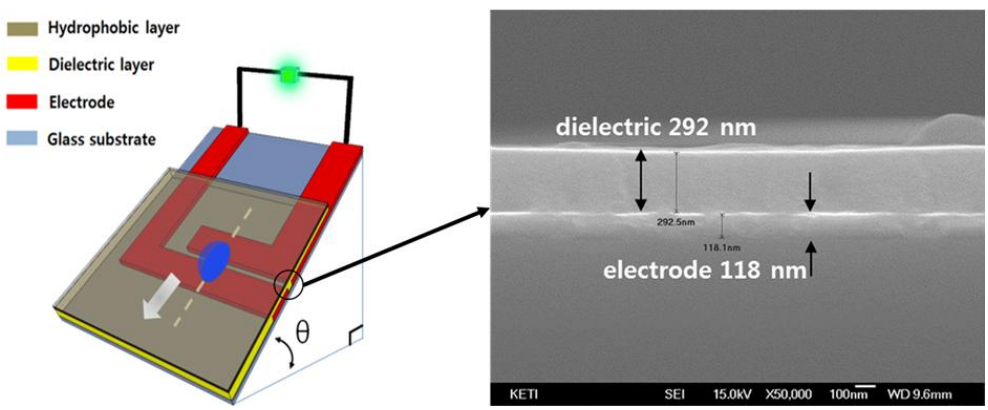

Figure 16. Schematic design of the WMAT and a cross-sectional SEM image on the glass substrate.

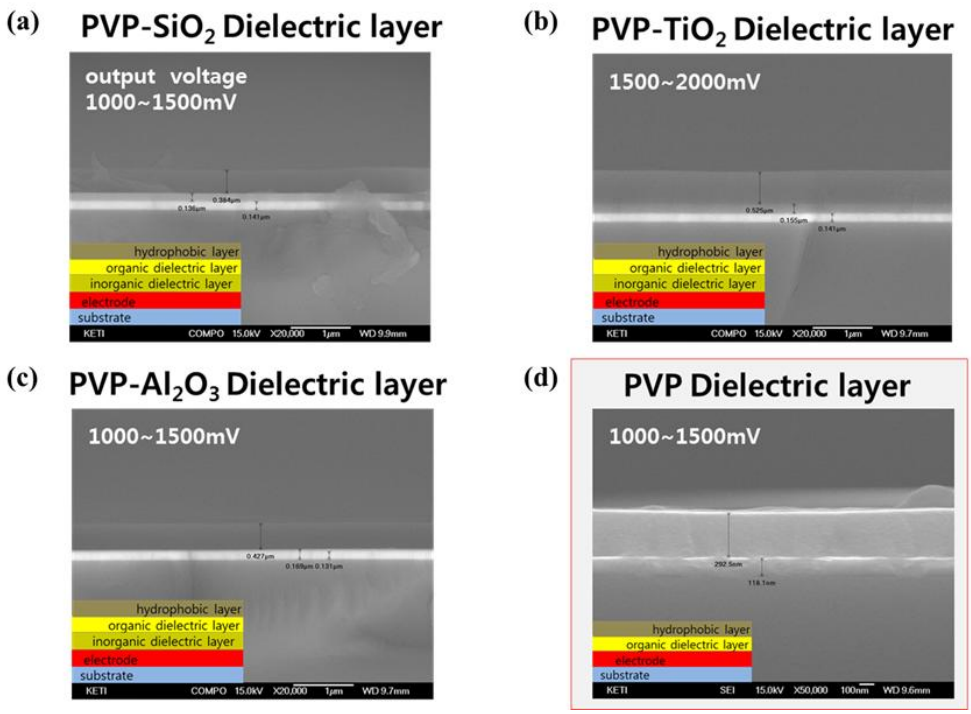

Figure 17. Cross sectional images of various WMAT structures.

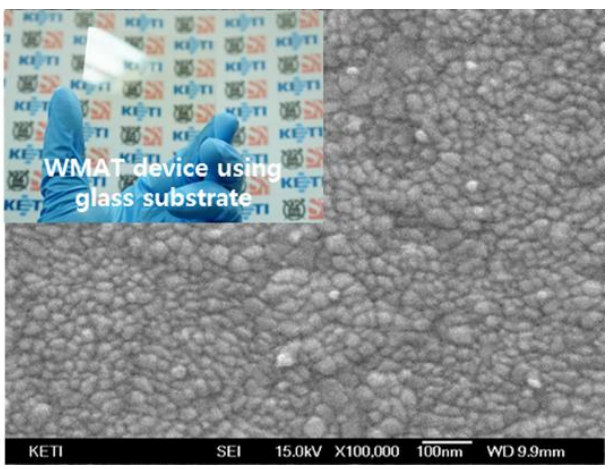

Figure 18. SEM image of WMAT surface treated by hydrophobic material.

3.3 Flowing Type WMAT

Figure 19 explained the fundamental and theoretical operating mechanism of flowing type WMAT. Water on hydrophobic layer played a role as an induction medium to attract the opposite charges of electrodes according to the variation of overlapping area between water and electrode.[23-25] The interfacial electrical capacitance was proportional to the overlapping area from the motion of water droplet.[26] In general, cations, anions, and water molecules, which were stimulated by the intrinsic polarity of PVP, were arranged on the interface of liquid/solid when liquid was placed on a solid surface.[27,28] Electrons were accumulated on the first capacitor,

$$Q_f \left(= C_f V_f = \varepsilon A_f V_f / d\right), \qquad (1)$$

and second capacitor,

$$Q_s \left(= C_s V_s = \varepsilon A_s V_s / d\right) , \qquad (2)$$

to keep an chemical potential balance of the surface according to overlapping area between water droplet and electrodes. Here, C_f and C_s are the capacitances of first electrode-droplet capacitor and second electrode-droplet capacitor, respectively. V_f and V_s are voltages on C_f and C_s, respectively. The effective electrical permittivity of the medium between dielectric layer and hydrophobic layer is ε. The sum of thickness of dielectric layer and hydrophobic layer is d. A_f and A_s are the overlapping areas of water droplet with first and second electrodes, respectively. For clear understanding, we explained mechanism of WMAT energy generation into 3 steps. The first step,

water droplet was charged positively in contact with the intrinsically negative charged PVP layer. EDL was created at the interface of the water droplet and PVP layer, so positive charges were accumulated on the first electrode to maintain electrical neutrality. Negative charges moved to the second electrode at the same time. The second step, the water droplet moved to the middle of the first and the second electrode. Overlapping areas of the water droplet with each electrode were equal. There was no charge transfer because C_f and C_s are same. The third step, water droplet fully covered the second electrode. The positive charges of the water droplet attracted negative charges of PVP layer. The negative charges of Q_s moved to the first electrode and finally they finished charge transfer between capacitors. When the water droplet started to overlap with second electrode and ended to overlap with first electrode, maximum peaks were shown since the difference of overlapping areas variation was the maximum. As a result on passing process of a water droplet between the electrodes, AC mode electric outputs were shown in Figure 20. The dominant output peaks of voltage and current were 3.1 V and 5.3 μA on average, which were enough to turn on a green LED. Figure 21 showed the experimental data measured by one water droplet passing (black dot) and numerical calculation data (red solid line), respectively. Through the comparison with experimental and theoretical data, WMAT proved its output characteristic of AC type device Figure 22 showed the real dimming image of LED light according to the variation of overlapping area between water droplet

and electrode. The output voltage and current were measured separately using digital multi-meter (NI 4070, National Instruments). Figure 23 showed the power density of WMAT. The output voltage and current were also detected by the voltmeter and ammeter connected to 80 kΩ load resistor in parallel and serial, respectively. The peak to peak power density was about 0.5 W/m^2 when the surface contact area of water droplet on substrate was 15.2 mm^2. Stability test for WMAT was performed for 1600 s (about 460 times) shown in Figure 23. The measured voltage showed that WMAT stably generated electricity for 1600 s. A water droplet with 30 μl volume was ejected at the rate of 10 ml per minute by the syringe pump. Droplets passed through the electrodes at speed of 0.4 m/s. The quantity of charge on the polymer film is calculated by as followed. In Figure 24 there is electrode-electrode capacitor with capacitance C_0. The ratio of two capacitance values is

$$\frac{C_E}{C_U + C_L} = \frac{\varepsilon_E \frac{A_E}{d_E}}{\varepsilon_U \frac{A_U}{d_U} + \varepsilon_L \frac{A_L}{d_L}} \fallingdotseq 10^{-5} \qquad (3)$$

$$C_{tot} = \frac{\varepsilon}{d} \frac{A_f A_s}{A_f + A_s}, \qquad (\because \varepsilon_f = \varepsilon_s \equiv \varepsilon,\ d_f = d_s \equiv d) \qquad (4)$$

Neglecting friction, the droplet's contact area with upper electrode is

$$A_2(t) = A_2(t=0) - \int h(x)dx \ \ ; x = x(t) = v_0 t + \frac{1}{2} g \sin\theta t^2 \quad (5)$$

$$= A_2(t=0) - R^2 \left[\cos^{-1}\left(\frac{d_0 - R}{R} \right) - \cos^{-1}\left(\frac{d_0 - R + x(t)}{R} \right) \right]$$

$$\left[+\left(\frac{d_0-R}{R}\right)\sqrt{1-\left(\frac{d_0-R}{R}\right)^2}+\left(\frac{d_0-R+x(t)}{R}\right)\sqrt{1-\left(\frac{d_0-R+x(t)}{R}\right)^2}\right] \quad (6)$$

Also, that with lower electrode is

$$A_3(t) = \int h(x)dx \quad (7)$$
$$= R^2\left[-\cos^{-1}\left(\frac{x(t)}{R}-1\right)+\sqrt{1-\left(\frac{x(t)}{R}-1\right)^2}\left(\frac{x(t)}{R}-1\right)+\pi\right]$$

R is the radius of a droplet.

Output voltage is given by following equation.

$$V = i(t)R_V, \quad (8)$$
$$i(t)(R_V+R_W) = V_f - V_s = \frac{d}{dt}\left(\frac{Q_f}{C_f}\right)-\frac{d}{dt}\left(\frac{Q_s}{C_s}\right)$$

Where i(t) that is flowing current when measured voltage is given by following equation. Where R_V and R_W are resistance across the voltmeter and the water droplet, respectively ($R_V \fallingdotseq 3R_W$). dQ_f and dQ_s are the electric charges variation in upper capacitor and lower capacitor, respectively, during the infinitesimal time, dt.

$$I(t) = \frac{V_f - V_s}{R_W} \quad (9)$$

As the droplet moved to the bottom the relative amount of overlapped area for each electrode varied according to the position of droplet. Since the speed of ions in the droplet is slower than that of the electrons in electrodes, there is potential variation in each capacitor. The different amount of electric charges variation in each capacitor made potential difference (V_f-V_s). The electric charges moved to the other electrode for neutralizing the potential difference.

As a result, on droplets passing between the electrodes, AC mode electric output was generated by the different variation rates between droplet's overlapped area with upper electrode and that with lower electrode. Here, $\varepsilon=5.1\varepsilon_0$, d = 290 nm, d_0 = 2 mm, R = 4.5 mm, A_f (t=0) = 15.90 mm^2, v_o = 0.5 ms^{-2}, g = 9.8 ms^{-2}, θ = 45°, R_V = 1 MΩ, R_W=320 kΩ where ε_0 electrical permittivity of vacuum.

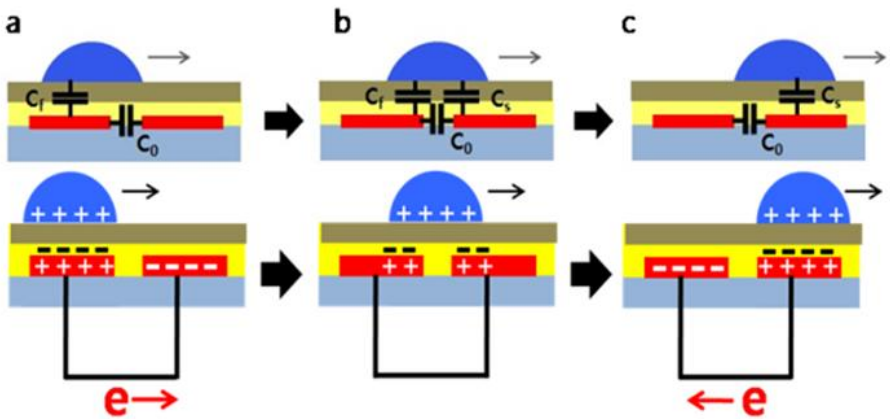

Figure 19. The fundamental operation principle of flowing type WMAT.

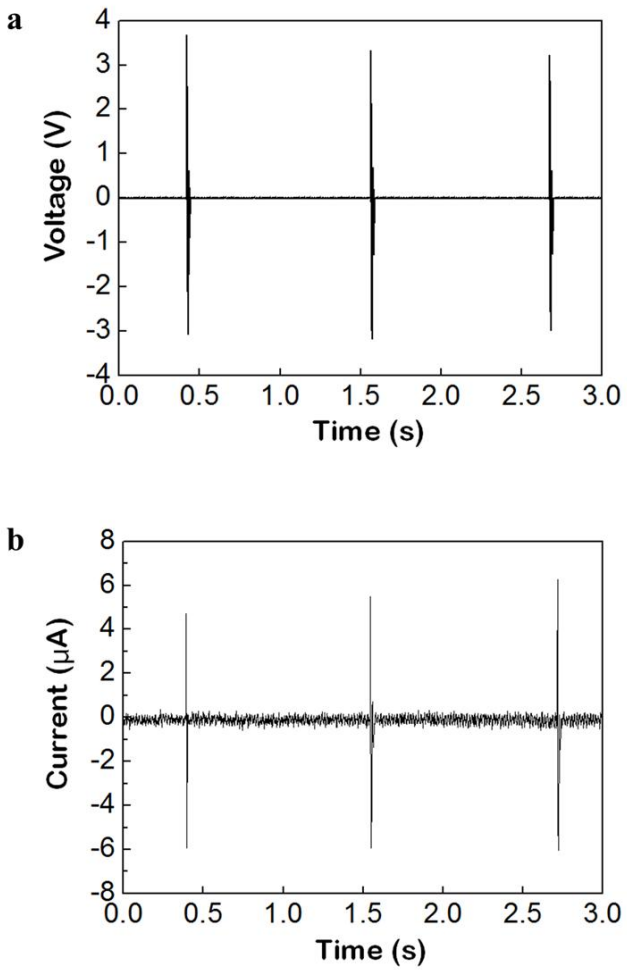

Figure 20. The measured output voltage and current of flowing type WMAT

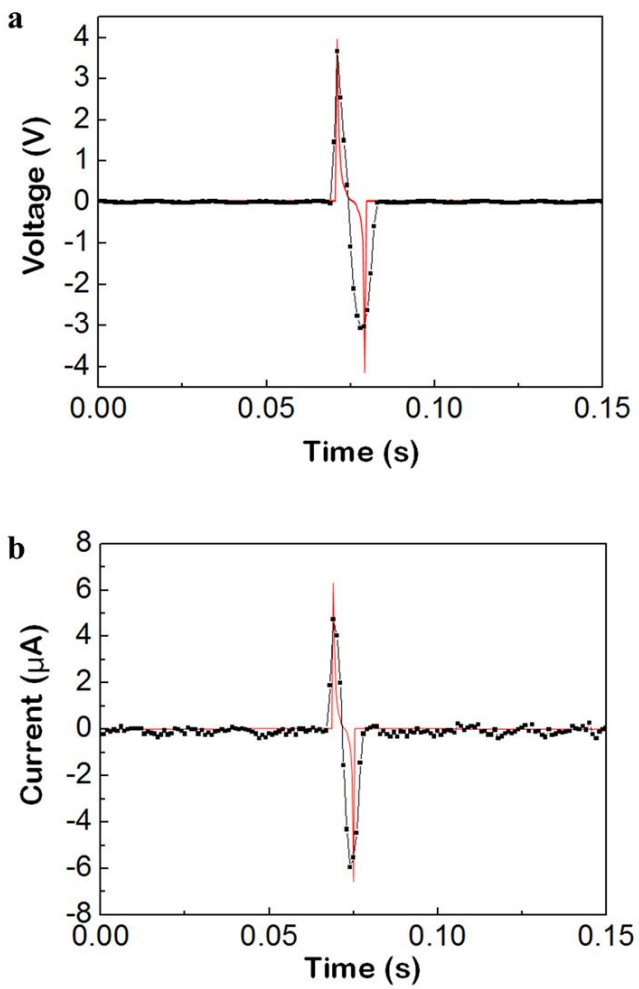

Figure 21. Comparison of calculation data (black dots) and experimental data (red solid line) of voltage and current.

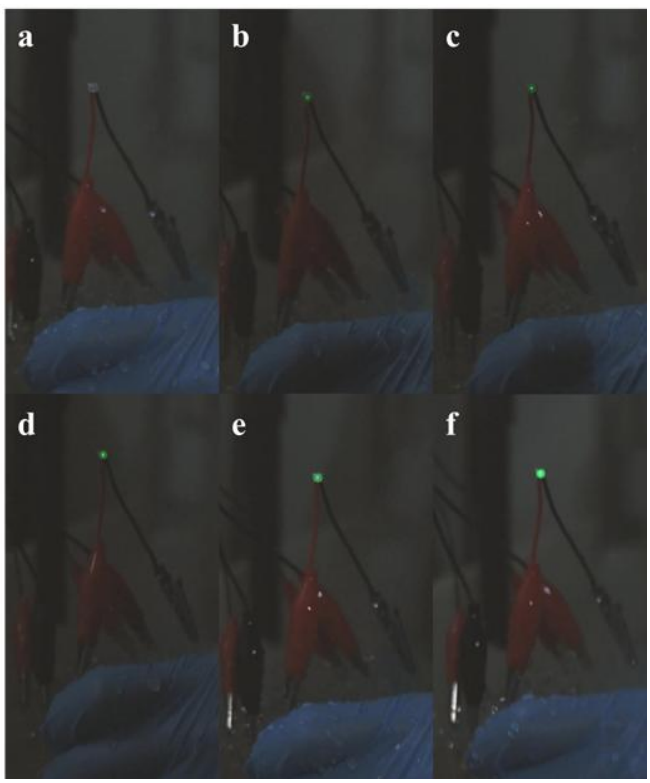

Figure 22. The real dimming image of LED light according to the variation of overlapping area between water droplet and electrode (a-f).

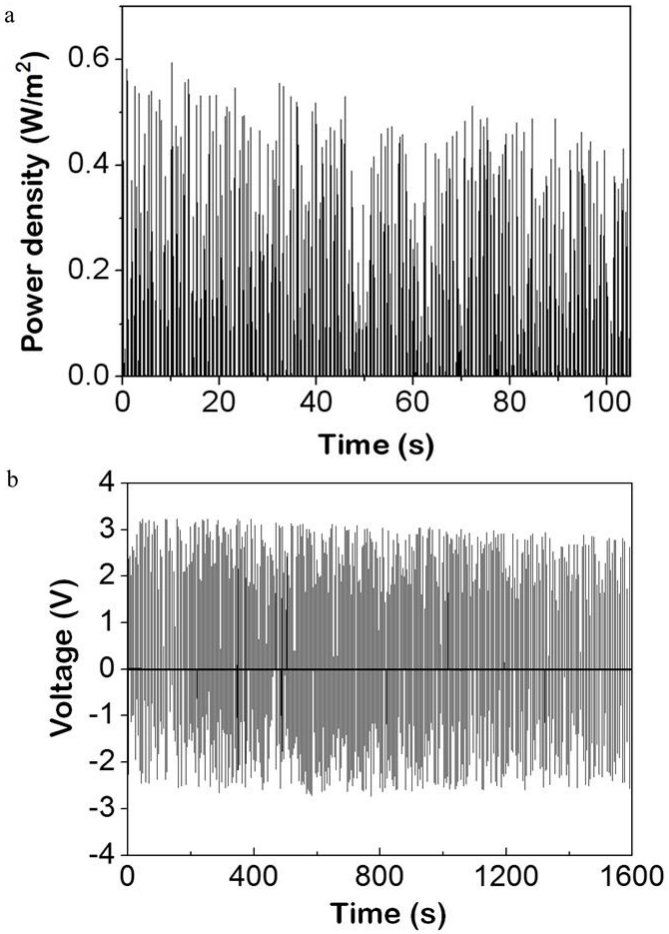

Figure 23. The power density and stability test of flowing type WMAT. Water droplets with 30 μL volume were ejected by the syringe pump at a rate of 10 mL min^{-1}. Droplets passed through the electrodes at a speed of 0.4 ms^{-1}. An 80 kΩ load resistor was used. The stability test for the WMAT was performed for 1600 s (about 460 times).

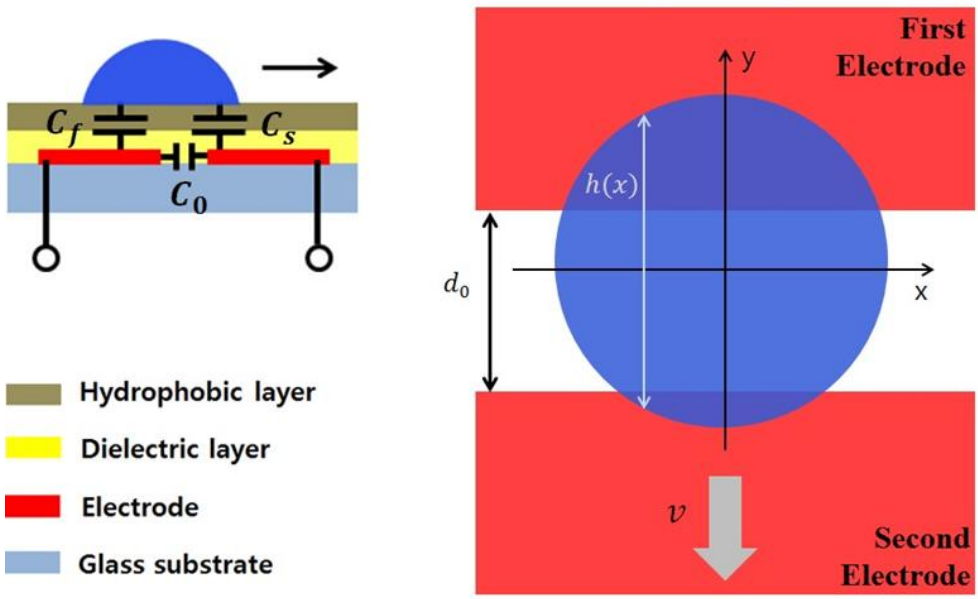

Figure 24. Schematic cross-section and top view image of device at the moment which droplet is located at around intermediate place between two electrodes. Assume droplet is a perfect sphere. h(x)is the droplet length of y-axis direction, $v = v_0 + g\sin\theta t$, where v_0 is initial velocity of droplet, g is acceleration of gravity, θ is tilted angle of device.

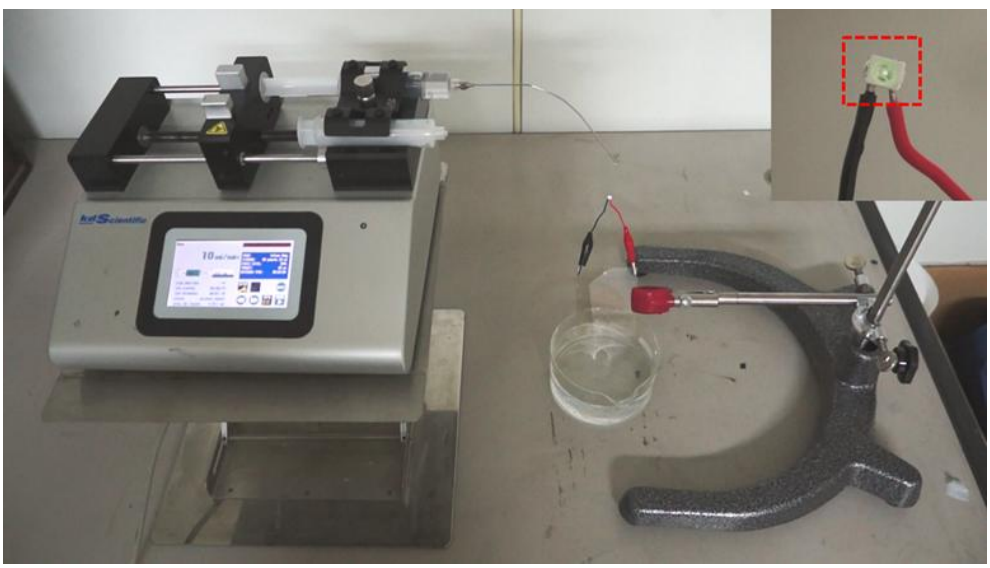

Figure 25. Experimental water droplet pumping equipment of flow type of WMAT.

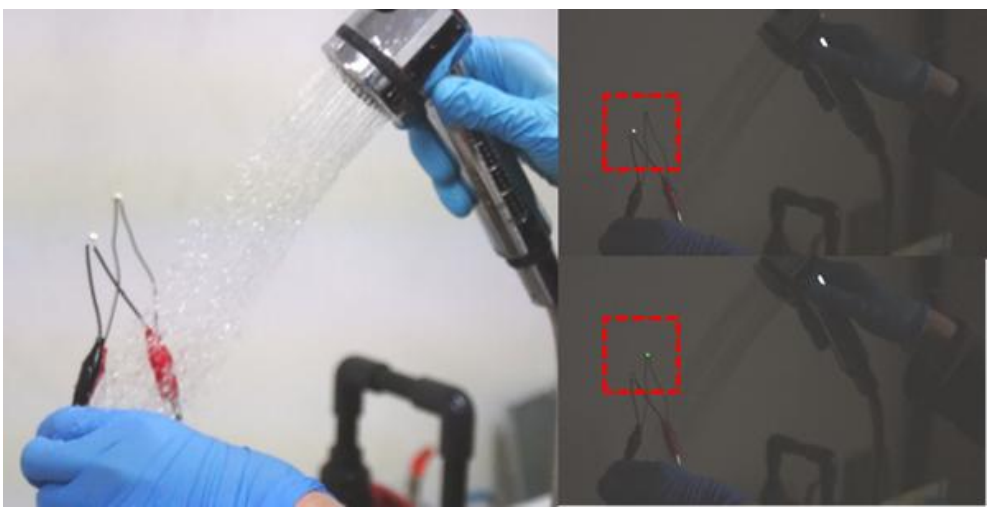

Figure 26. LED lighting capture image powered by flowing type WMAT with water-jet equipment.

3.4 Pushing & Dipping Type WMAT

By extension, we introduced this energy harvesting concept to the energy generation from the fluctuations of water contact area. Figure 27 illustrated the design and the mechanism of pushing/releasing type of WMAT. This type of WMAT used two asymmetric plates. One was composed of ITO glass, PVP layer and hydrophobic layer, and the other was composed of hydrophobic layer coated on ITO glass. Flow of electrons was not occurred until the water droplet contacted with top substrate shown in equilibrium state.[29,30] For the pushing process (Figure 27, middle), the water droplet was flattened, height D2, and its contact area on plates was also increased. Since the density of EDL made on the bottom plate was much larger than that of EDL on top plate due to the intrinsically negative-charged dielectric PVP layer, the electrons moved to the bottom electrode. Thus, electrical currents flowed through the circuit. In the releasing process (Figure 27, right), height D1, droplet was perfectly restored to its initial form, and the electrons accumulated on the bottom electrode went back to the top electrode so that the AC mode electric current was generated in the circuit. A water droplet with 100 μl volume was periodically flattened at the rates of 120 rpm (revolutions per minute) by the machine. The measured output voltage (Figure 28 a) and current (Figure 28 b) were generated from pushing/releasing motion of water droplet. Here, through the difference of charge density on WMAT with two asymmetric plates, we fully turned on a green LED by one-cycle pushing/releasing motion with a single

droplet. The maximum output peaks of voltage and current averaged at 6 V and 70 μA from the motion of single droplet. The main factor to determine the output voltage and current is the contact area in our WMAT system. Also the goal of our research is to find out the relation between electrical output and contact area of water droplet on electrode. Figure 29 is the comparison of the size of water droplet with flowing type of WMAT and the size of water droplet with pushing/releasing type of WMAT (diameter of released state : 6mm, pushed state : 28 mm). So the electrical output of pushing type was far large than that of flowing type. The difference of a far large contact area between pushing type and flowing type is shown in Figure 29. Since larger contact area lead more charges to the electrodes, the output current of pushing/releasing type was much large than that of flowing type. Figure 30 shows the variation of the output voltage and the current of pushing type WMAT according to the increase of number of droplets, and the change of voltage value of pushing type WMAT with the change of revolutions per minute (RPM). This is novel and distinguishing feature of WMAT that electrical output value is proportional to contact area and velocity between water droplet and electrode differ from triboelectrics. This result is a common phenomenon for energy harvesting methods using EDL operating principle. In our reliability experiment, we could confirm the falling tendency of output voltage according to evaporation of water droplet. Also, output voltage measured according to the ionic concentration showed negative correlation tendency shown

in Figure 31. Since ions screened the potential difference between the capacitors, lower electrical signal is generated by water which have higher NaCl concentration.[31] The adhesion of ions on substrate is main factor to low the output voltage. We compared the results of distilled water, salted water and tap water again. There was minor difference of output voltage showed in Figure 32. Zong-Hong Lin et al. have recently reported that energy harvesting device using water was affected by the ion concentration.[32] However the main factor to determine the electrical energy is the variation of overlapping area between water droplet and electrode. The ionic concentration of water only influenced tiny value of electrical output compare to the variation of overlapping area. So we skipped the effect of ionic concentration in this study. We mainly considered the overlapping area related with variable capacitance. Other several factors which may affect the amount of electrical generation, such as the variation of ionic concentration, the variation speed of contact area, the dielectric constant of dielectric layer, surface morphology, flow speed, and structure of device, will be studied in the future research. Figure 33 showed the stability test considering natural water evaporation.

Figure 34 showed the dipping type of WMAT imitating the natural fluctuation of sea and river. This type of WMAT used two asymmetric plates. In dipping, the surface of WMAT contacted with water. EDL was created at the interface between PVP layer and water. The water was positively charged due to the negative-charged PVP layer at EDL system. The first electrode was charged positively,

so negative charges transferred from the second electrode to the first electrode. When each substrate was taken out of water, the electrical equilibrium was broken. So, negative charges moved from the second electrode to the first electrode shown in below diagram. Figure 34 (b) indicated the example of practical application to use energy harvester via natural water fluctuation motion such as sea wave and river slapping. Even though this WMAT was just infant, the generated electric power was enough to turn on a green LED. Figure 35 showed the generated voltage and current, respectively.

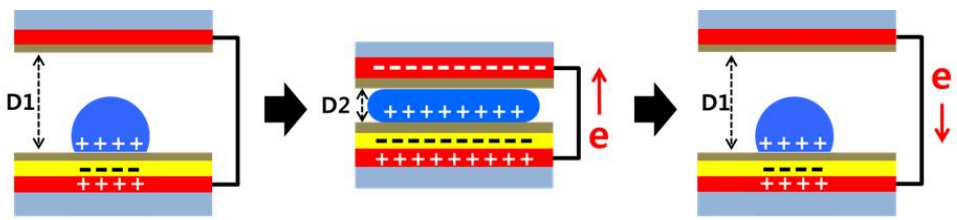

Figure 27. The fundamental operation principle of pushing type WMAT.

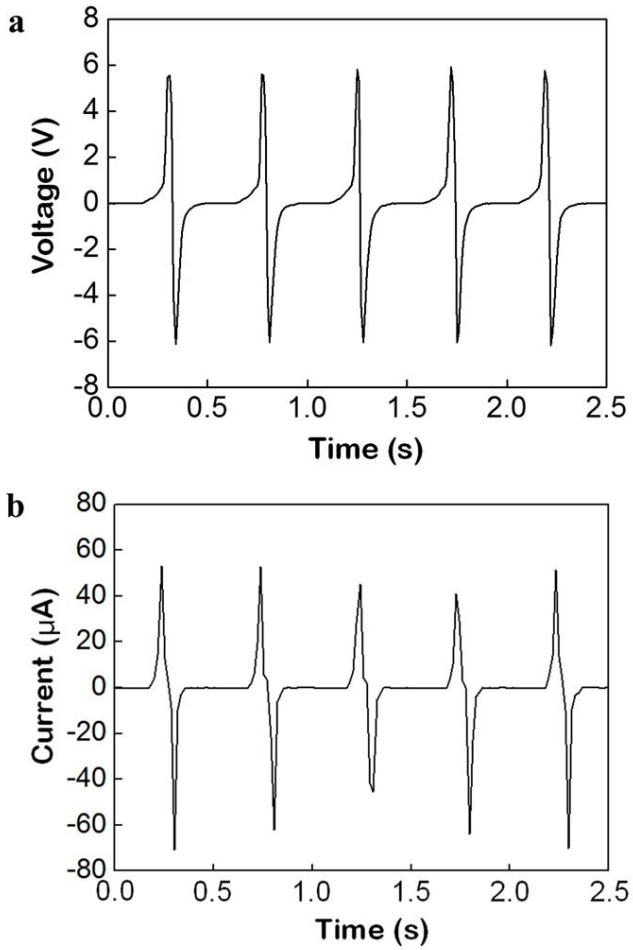

Figure 28. The measured output voltage (a) and current (b) of pushing type WMAT.

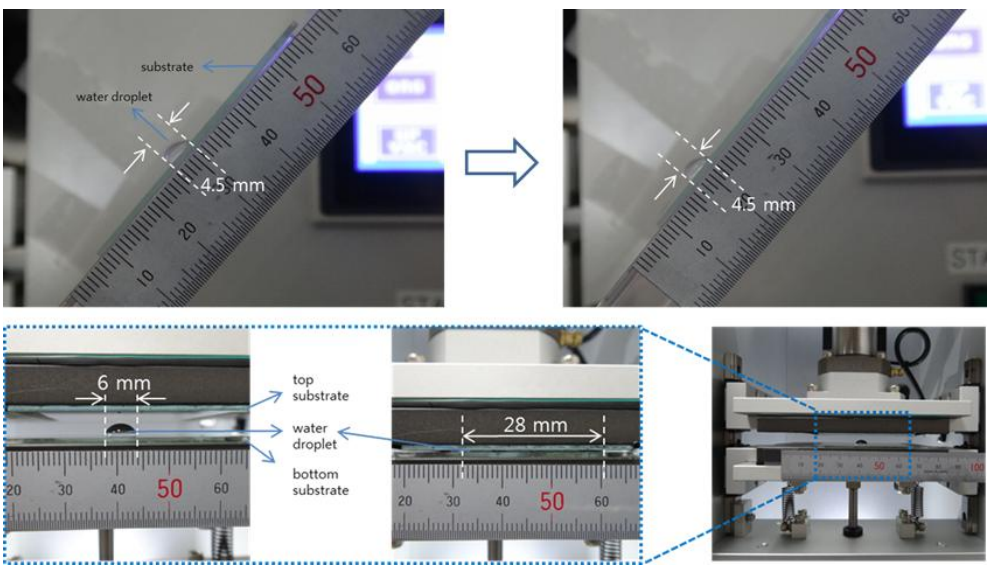

Figure 29. The comparison of the size of water droplet with flowing type of WMAT and the size of water droplet with pushing/releasing type of WMAT (diameter of released state : 6 mm, pushed state : 28 mm) and pushing/releasing machine used in this experiment.

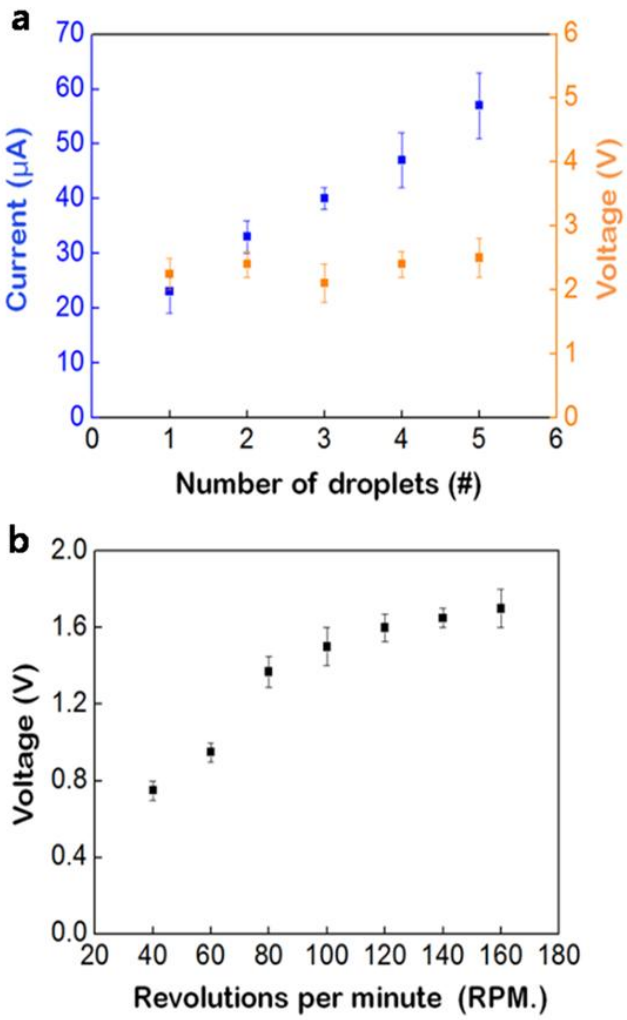

Figure 30. (a) The variation of the output voltage and the current of pushing type WMAT according to the increase of number of droplets, (b) the change of voltage value of pushing type WMAT with the change of revolutions per minute (RPM).

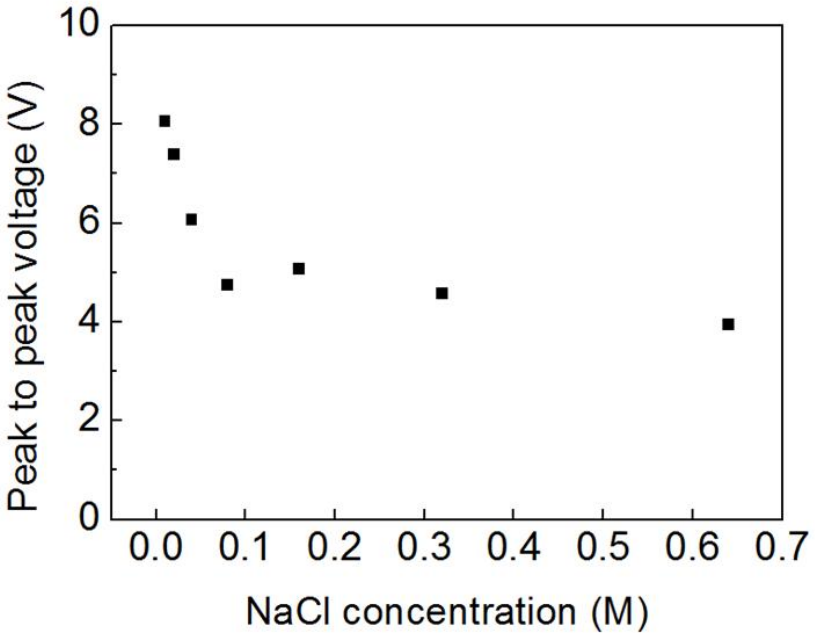

Figure 31. The comparison of voltage output according to the NaCl concentration measured by pushing/releasing motion.

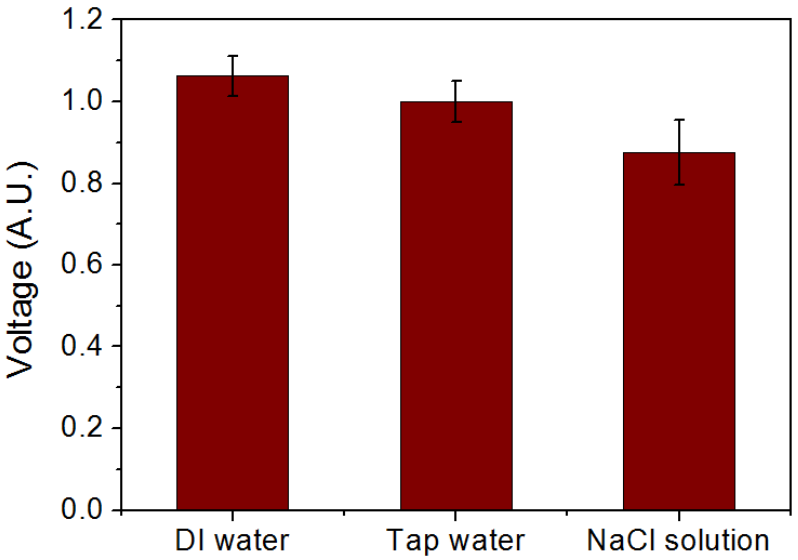

Figure 32. The comparison of voltage output DI water, Tap water and NaCl solution. Measured by pushing/releasing motion.

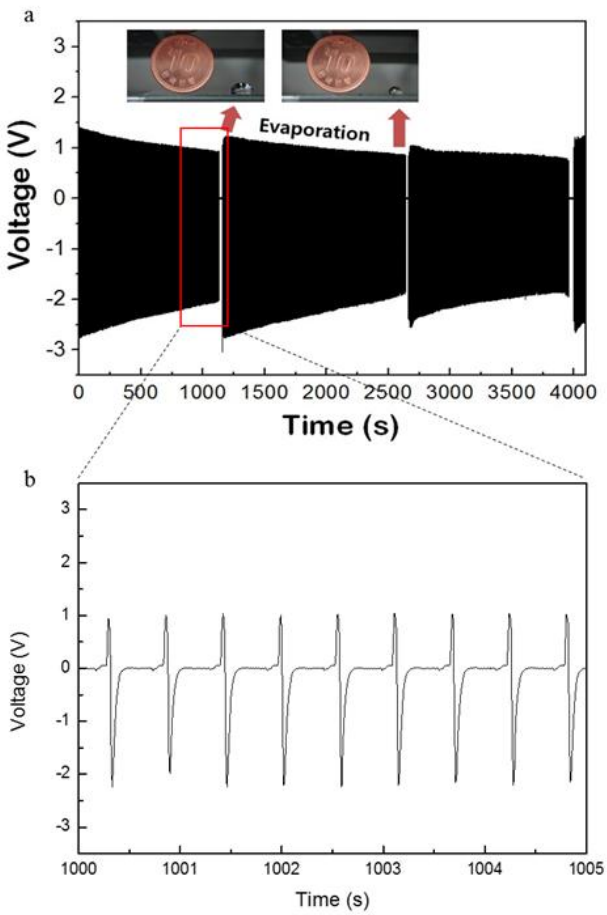

Figure 33. (a) Output voltage was measure by pushing/releasing motion. A water droplet with 100 μl volume was periodically flattened at the rate of 100 rpm (revolutions per minute). Inset images show initial droplet (100 μl) and evaporated droplet (~40 μl). (b) Magnified voltage peaks of stability experiment.

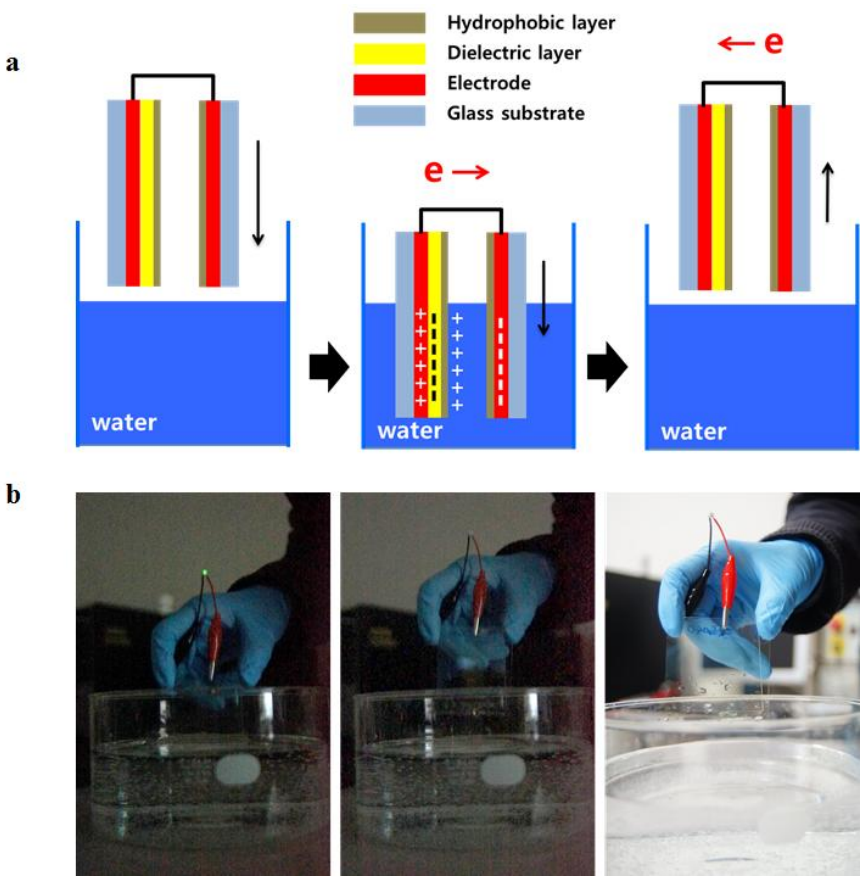

Figure 34. Design and mechanism for dipping type of WMAT. (a) Schematic cross-sectional design and basic mechanism for generating electricity. The measured output voltage (b) green LED turn on image using dipping type WMAT.

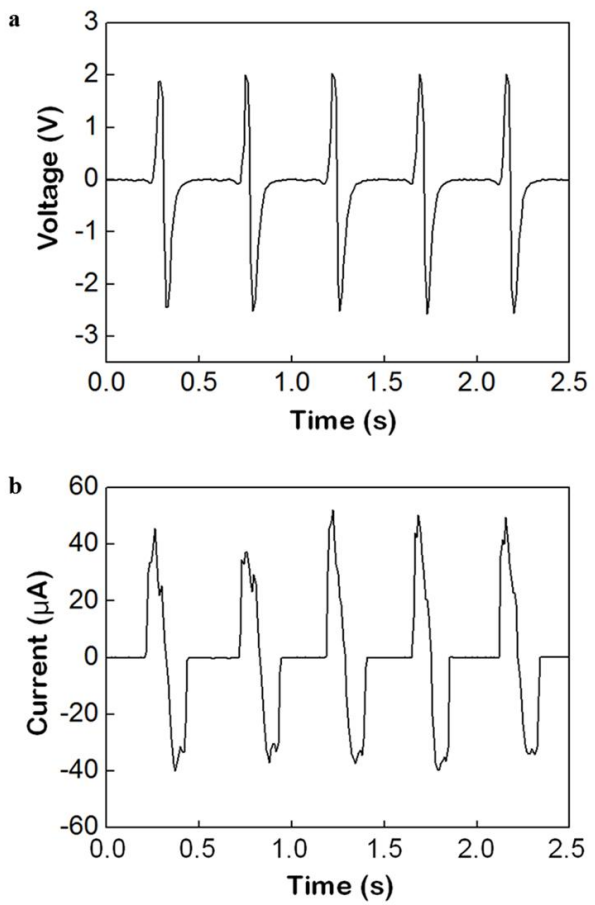

Figure 35. The measured output voltage (a) and current (b) of dipping type WMAT.

3.5 Fabrication of WMAT by Solution Process

The For WMAT using flowing water, the ITO layer was etched with HCl for electrode patterning. In pushing/releasing type WMAT was not etched. PVP which was a blend of Poly (4-vinylphenol), Propylene glycol monomethyl ether acetate, and Poly (melamine-co-formaldehyde) methylated/butylated (Sigma aldrich) with mass ratio 2:1:17 was spin-coated at 3000 rpm for 35 s (acceleration speed at 500 rpm for 2 s) after ultraviolet ozone (UVO, λ = 185 and 254 nm, 100 mW/cm2) exposure for 30 min, and then dried at 200 °C for 20 min. To prevent water droplet from attaching to the substrate, EKG-6015 (ETC company, Germany) was spin-coated at 4000 rpm for 35 s (acceleration speed at 500 rpm for 2 s) after UVO (λ = 185 and 254 nm, 100 mW/cm^2) exposure for 30 min and then dried at 200 °C for 15 min.

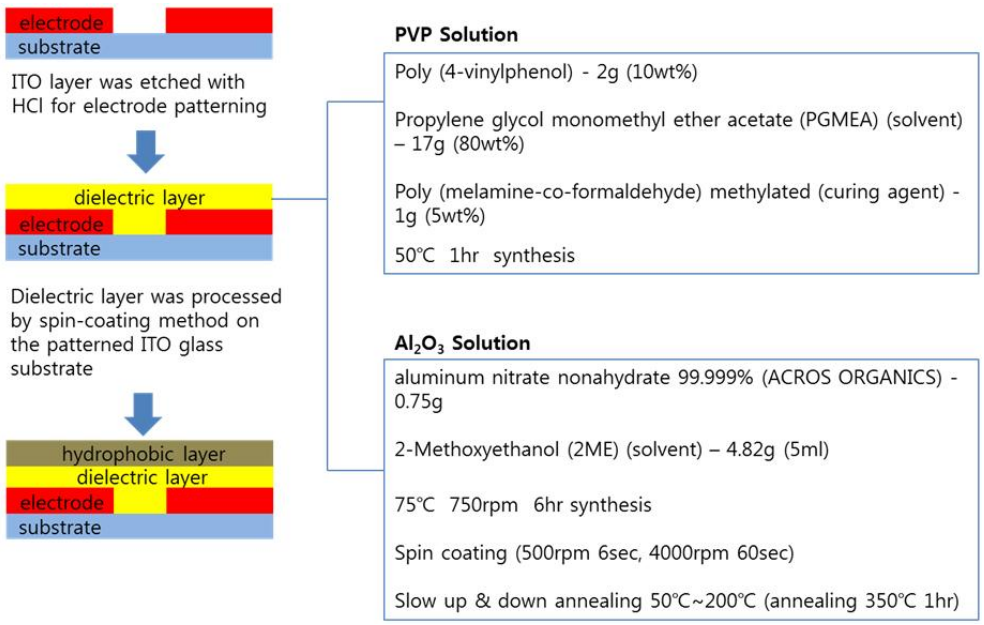

Figure 36. The fabrication of WMAT by solution process.

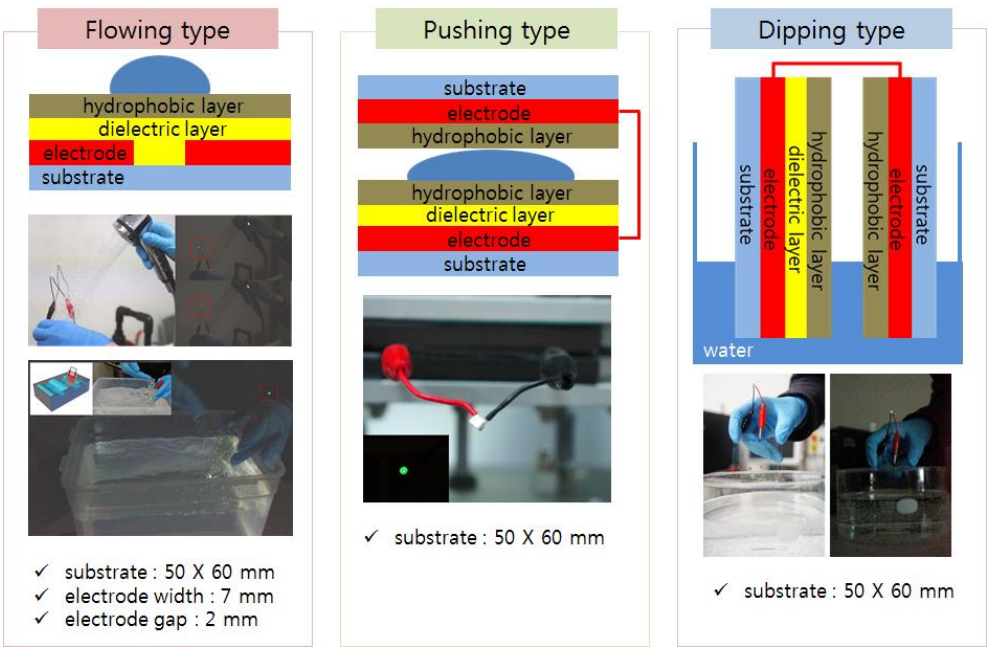

Figure 37. The structures and dimensions of various WMAT.

3.6 Performance characterization of WMAT

The morphology of the hydrophobic layer surface and the cross-section of the dielectric layer was investigated using a field emission scanning transmission electron microscope (FE-SEM) (JSM-7000F, JEOL). To operate the pushing/releasing motion, a pushing machine was made autonomously. The water flow was ejected using a syringe pump (Legato 200, KdScientific Inc.) The output voltage and current were detected by using 61/2-digit digital multi-meter and 1.8 MS/s isolated digitizer (NI 4070, National Instruments). 100 data points were obtained in one second. Voltmeter or ammeter was connected directly to the electrodes to detect electric signals. The water droplets dripped onto the centre of the first electrode tilted at an angle of 45° to the horizontal. The water droplets passed through the electrodes at speed of 0.4 m/s.

3.7 Conclusions

In summary, we demonstrated the WMAT successfully generates electricity enough for turn on the LED light in real time from various natural water motions such as flowing, pressing, dipping, and slapping. We designed the WMAT with the simple structure consist of one PVP dielectric layer and one hydrophobic layer on electrodes. This simple structure has considerable advantages in process and manufacturing cost. All fabrication processes of WMAT were solely conducted by solution process without any vacuum and high-cost process. This simple and low-cost process is the most attractive one among the advantages of WMAT in comparison with other energy harvester with complex structure and cumbersome process. With the variation of overlapping areas between water and electrodes, this energy transducer could enough convert the energy of water's mechanical motion to electric energy. In this study, we mainly considered the overlapping area related with variable capacitance, but the amount of electrical generation depends on the several factors, such as the dielectric constant of dielectric layer, surface morphology, flow speed, and structure of device. These issues will be studied in the future research. Although WMAT is just in its infancy in comparison with other energy harvesting and transducing devices, but we believe that it is a good attempt to explore new application area of energy conversion. This concept of energy transducing using various water motion have a possibility for energy harvester using various discrete water motion such as rain, sea wave, and home

water flushing.

- One of the significant limitations to apply capacitive-transducer to energy harvester is to need external bias-voltage source for accumulating charges at electrodes. However, herein we introduce the novel active capacitive-transducer without any external bias-voltage sources using water motion.

- We found that the overlapped area variation between the water and the dielectric layer can effectively induce the variation of electric charges, and then easily generate electricity.

- This concept of energy transducing using various water motion have a possibility for energy harvester using various discrete water motion such as rain, sea wave, and home water flushing.

- All fabrication processes of WMAT were solely conducted by solution process without any vacuum and high-cost process.

- The motion of water droplet of 30 μl, we could successfully generate the electricity with a peak voltage ~3.1 V and peak current ~5.3 μA, which was enough to turn on a green LED.

3.8 References

1 Li, Dongqing, "Electrokinetics in microfluidics" Vol(2), Academic Press, 2004.

2 Chang, Hsueh-Chia, and Leslie Y. Yeo, "Electrokinetically driven microfluidics and nanofluidics", Cambridge University Press, 2010.

3 Parsons, Roger, "The electrical double layer: recent experimental and theoretical developments", Chem. Rev, 90(5), 1990, 813-826.

4 Schoch, Reto B, Jongyoon Han, and Philippe Renaud, "Transport phenomena in nanofluidics", Rev. Mod. Phys, 80(3), 2008, 839.

5 Levine, S, and Graham H. Neale, "The prediction of electrokinetic phenomena within multiparticle systems", J Colloid Interface Sci, 47(2), 1974, 520-529.

6 Zeng, S, Chen, C. H, Mikkelsen, J. C, & Santiago, J. G, "Fabrication and characterization of electroosmotic micropumps", Sens Actuators B Chem, 79(2), 2001, 107-114.

7 GGuo, W, Cao, L, Xia, J, Nie, F. Q, Ma, W, Xue, J, "Energy Harvesting with Single Ion Selective Nanopores: A Concentration Gradient Driven Nanofluidic Power Source", Adv Funct Mater, 20(8), 2010, 1339-1344.

8 Brogioli, D, R. Zhao, and P. M. Biesheuvel, "A prototype cell for extracting energy from a water salinity difference by means of double layer expansion in nanoporous carbon

electrodes", Energy Environ Sci, 4(3), 2011, 772-777.

9 Lin, Z. H, Cheng, G, Lin, L, Lee, S, & Wang, Z. L, "Water - Solid Surface Contact Electrification and its Use for Harvesting Liquid Wave Energy", Angew Chem Int Ed Engl, 52(48), 2013, 12545-12549.

10 Moon, J. K, Jeong, J, Lee, D, & Pak, H. K, "Electrical power generation by mechanically modulating electrical double layers", Nat Commun, 4, 2013, 1487.

11 Jean-Mistral, C., T. Vu Cong, and A. Sylvestre, "Advances for dielectric elastomer generators: Replacement of high voltage supply by electret", Appl Phys Lett, 101(16), 2012, 162901.

12 YoungJun Yang, Junwoo Park, Soon-Hyung Kwon and Youn Sang Kim, "Fluidic Active Transducer for Electricity Generation", Sci. Rep, 5, 2015.

13 Beeby, S. P, M. J Tudor, and N. M. White, "Energy harvesting vibration sources for microsystems applications", Meas Sci Technol, 17(12), 2006, 175.

14 Sodano, Henry A, Daniel J. Inman, and Gyuhae Park, "A review of power harvesting from vibration using piezoelectric materials", Shock Vib Digest, 36(3), 2004, 197-206.

15 Wang, Zhong Lin, and Jinhui Song, "Piezoelectric nanogenerators based on zinc oxide nanowire arrays", Science 312(5771), 2006, 242-246.

16 Mitcheson, P. D, Yeatman, E. M, Rao, G. K, Holmes, A. S, &

Green, T. C, "Energy harvesting from human and machine motion for wireless electronic devices", Proceedings of the IEEE, 96(9), 2008, 1457-1486.

17 Guigon, R, Chaillout, J. J, Jager, T, & Despesse, G, "Harvesting raindrop energy: experimental study", Smart Mater Struct, 17(1), 2008, 015039.

18 Erturk, A, Vieira, W. G. R, De Marqui Jr, C, & Inman, D. J, "On the energy harvesting potential of piezoaeroelastic systems", Appl Phys Lett, 96(18), 2010, 184103.

19 Krupenkin, Tom, and J. Ashley Taylor, "Reverse electrowetting as a new approach to high-power energy harvesting", Nat Commun, 2, 2011, 448.

20 Gordon, J. M, "Generalized power versus efficiency characteristics of heat engines: the thermoelectric generator as an instructive illustration", Am. J. Phys, 59(6), 1991, 551-555.

21 Wang, Z, Leonov, V, Fiorini, P, & Van Hoof, C, "Realization of a wearable miniaturized thermoelectric generator for human body applications", Sens. Actuator A: Phys, 156(1), 2009, 95-102.

22 Glynne-Jones, Peter, Stephen Paul Beeby, and Neil M. White, "Towards a piezoelectric vibration-powered microgenerator", IEE Proceedings-Meas. Sci. Technol, 148(2), 2001, 68-72.

23 Yıldırım, Ender, and Haluk Külah, "Electrostatic energy harvesting by droplet-based multi-phase microfluidics" Microfluid Nanofluidics, 13(1), 2012, 107-111.

24 Lin, Z. H, Cheng, G, Lee, S, Pradel, K. C, & Wang, Z. L, "Harvesting Water Drop Energy by a Sequential Contact Electrification and Electrostatic Induction Process", Adv Mater, 26(27), 2014, 4690-4696.

25 Su, Y, Wen, X, Zhu, G, Yang, J, Chen, J, Bai, P, "Hybrid triboelectric nanogenerator for harvesting water wave energy and as a self-powered distress signal emitter", Nano Energy, 9, 2014, 186-195.

26 Paek, Eunsu, Alexander J. Pak, and Gyeong S. Hwang, "A computational study of the interfacial structure and capacitance of graphene in [BMIM][PF_6] ionic liquid", J Electrochem Soc, 160(1), 2013, A1-A10.

27 Hu, W, Haddad, P. R, Hasebe, K, Tanaka, K, Tong, P, & Khoo, C, "Direct determination of bromide, nitrate, and iodide in saline matrixes using electrostatic ion chromatography with an electrolyte as eluent", Anal. Chem, 71(8), 1999, 1617-1620.

28 Wang, Hainan, and Laurent Pilon, "Accurate simulations of electric double layer capacitance of ultramicroelectrodes", J Phys Chem C, 115(33), 2011, 16711-16719.

29 Davis, James A, Robert O. James, and James O. Leckie, "Surface ionization and complexation at the oxide/water interface", J Colloid Interface Sci, 63(3), 1978, 480-499.

30 Grahame, David C, "The electrical double layer and the theory of electrocapillarity", Chemical reviews, 41(3), 1947, 441-501.

31 Fedorov, Maxim V, and Alexei A. Kornyshev, "Towards

understanding the structure and capacitance of electrical double layer in ionic liquids", Electrochimica Acta 53(23), 2008, 6835-6840.

32 Zong-Hong Lin, Gang Cheng, Long Lin, Sangmin Lee, and Zhong Lin Wang. "Water - Solid Surface Contact Electrification and its Use for Harvesting Liquid Wave Energy." Angewandte Chemie International Edition 52.48 , 2013, 12545-12549.

Chapter 4. Fabric-based Water Motion Active Transducer

4.1 Overview

The recent trend of energy harvesting device is an adoption of fabric materials with flexible and stretchable according to the increase of wearable electronics.[1-3] But it is a difficult process to form a core structure of dielectric layer or electrode on fabric materials.[4] In particular, a fabric-based energy harvesting device in contact with water has not been studied though there are many challenging issues including an insulation and water absorption in harsh environment.[5,6] So we propose an effective method to obtain an electrical energy from the water contact using our new fabric energy harvesting device. Our water motion active transducer (WMAT) is designed to obtain electrical energy from the variable capacitance through the movement and contact of water droplet. In this paper, we succeeded in generating an electrical energy with peak to peak power of 280 μW using a 30 μl of water droplet with the fabric WMAT device of 70 mm X 50 mm dimension. Furthermore, we specially carried out spray coating and transfer processes instead of conventional spin coating process on fabric materials to overcome the limitation of its uneven morphology, porous and deformable assembly. Recently, the needs of the wearable device shows a significant increase on the back of the successful debut for various light and small electronics

which change our paradigm about conventional electronics from portable to wearable.[7,8] Energy harvesting devices also have been developed using a wearable fabric material for keeping up with the advanced technology.[9,10] Light and wearable energy harvesting device is attached to the human body for a variety of purposes, such as heart rate sensor, movement sensors and energy consumption sensors.[11-13] Basic material is an important factor to determine the electrical performance and durability in these devices. Flexibility, stretchiness and light weight are core conditions requested by wearable device market.[14] At this moment, various fabric materials receive attention from the most promising candidate for wearable electronics. Actually, fabric is a very familiar material with human for thousands of years because of its deformable, durable, washable, flexible and stretchable merits.[15] On the other hand, these features only act as a positive effect for a cloth, but a negative effect for an electronic devices. Most semiconductor-based processes of deposition and patterning are targeted at flat and rigid substrate made of glass or wafer. So far energy harvesting devices using fabric material are based on piezo effect, triboelectric, seebeck effect technologies.[16-18] Unfortunately, these technologies are many limitations to realize the fabric-based energy harvesting device and to select fabric material for their complex and sensitive process conditions as like high temperature, spin coating process, annealing process, passivation layer from oxygen and moisture. Some research groups realized fabric-based energy harvesting device using piezo-electronic

technology, but still showed tiny electrical output power not enough for lighting. Piezo nano-generator composed of sandwich structure mixed by poly-vinylidenefluoride (PVDF)-$NaNbO_3$ nano-composite and conductive fabric electrode was reported.[19] Another research group showed fiber-based electrification device of smart garments for monitoring physiological and bio-mechanical signals of the human body.[20,21] General energy harvesting devices are vulnerable to contact with water as well as electrical products. Most electronics without waterproof treatment tend to deteriorate or fail in contact with water condition. However, the needs of reliable energy generation technology have been requested in emergency situation which is permitted only independent power system for human safety under water contact environment. For this reason, energy harvesting method using water also was reported several times. Energy harvesting using water motion is the one of the new trends of the generating of electricity. Kim's research team reported electrical double layer (EDL) was the main factor to generate electricity when water droplet contacted with polymer substrate and demonstrated pushing-releasing type and flowing type energy harvesting device enough to LED turn on.[22] Moon's group also found that the mechanically vibrating water droplet with variation of contact area caused the electrical current.[23] Additionally, electrification of water is understood for generating the electricity. Miljkovic et al. studied that jumping water droplet with net charge was used an energy source of harvesting system.[24] Wang's research team designed solid-water contact electrification

energy harvesting device consist of nano-patterned polymer film and metal layer.[25] However, these water-based energy harvesting devices also need to modify the material and process suitable for fabric-based applications. Their core materials must be changed from rigid to flexible and stretchable material and photo-lithography based process also be replaced by new process compatible with various three-dimensional structures. Here, we propose fabric-based WMAT which has an advantage of flexible, stretchable, wearable feasibility and an excellent electrical output using natural water motion including unfavorable environment unable to apply the general energy harvesting device. In our previous report, we demonstrated that WMAT of glass substrate generated enough electricity to turn on a LED light using various water motions, such as flowing, pressing, dipping and slapping.[26,27] In this research, we studied an effective fabrication method using newly adopted fabric-based materials and polymer materials to find easy and simple method differ from the conventional complex process. Furthermore, we carried out spray coating and transfer process with fabric material to overcome the limitation of spin coating and lithography process of high temperature and chemical treatment. We verified polyurethane, poly-methyl methacrylate (PMMA) layers using spray coating process are effective dielectric layer and energy conversion layer on the fabric substrate in our WMAT structure. To achieve final demonstration, fabric WMAT was detached from a rigid substrate after core process and was attached to a polyester substrate using transfer process after

all spray process. Unlike the other complex and sensitive energy harvesting devices, our fabric WMAT has an advantage of physical bending and folding characteristic because all materials are flexible and affordable fabrics.

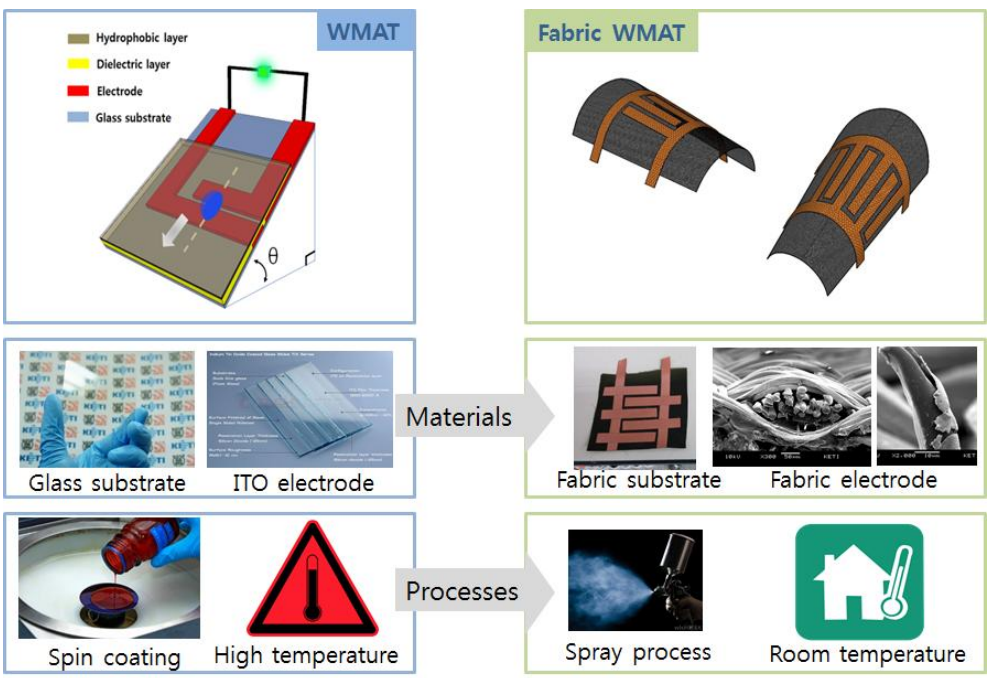

Figure 38. The difference of core material and process between WMAT and Fabric WMAT.

4.2 Structure & Material of Fabric WMAT

Fabric WMAT has a similar structure with our previous glass-based WMAT but core material is changed suitable for fabric-based process. Fabric WMAT consists of copper-plated polyester electrode, polyester substrate, polymer dielectric layer, waterproof layer and hydrophobic layer. Fabric electrodes are plated with copper with polyester yarns. Polyester textile and polyurethane are utilized as a substrate and as a waterproof material, respectively. PMMA and poly-4-vinyl phenol (PVP) is used for a dielectric layer causing capacitance variance. Nano silica dispersed liquid is introduced as a hydrophobic layer. Figure 39 shows the conceptual diagram and cross-sectional SEM image of fabric WMAT. Fabric WMAT is fabricated on the polyester substrate with fabric electrode, polyurethane waterproof layer, polymer energy conversion layer and hydrophobic layer. Ladder-shaped electrodes are designed by allowing the size of water droplet and increasing the possibility of overlapping area between electrodes and irregular water droplets. So the arrangement of upper and lower electrode has a repeatable pattern at regular intervals of 3 mm. In addition to repeatable electrodes are positioned with parallel integration to prevent superposition of output pulse from falling of water droplets. Figure 39 indicates cross-section of close-woven copper plated polyester yarns after polyurethane solution spray treatments. Many air gaps and rugged surface are filled with polyurethane solution and observed by scanning transmission electron microscopy (SEM, JSM-700F, JEOL) analysis.

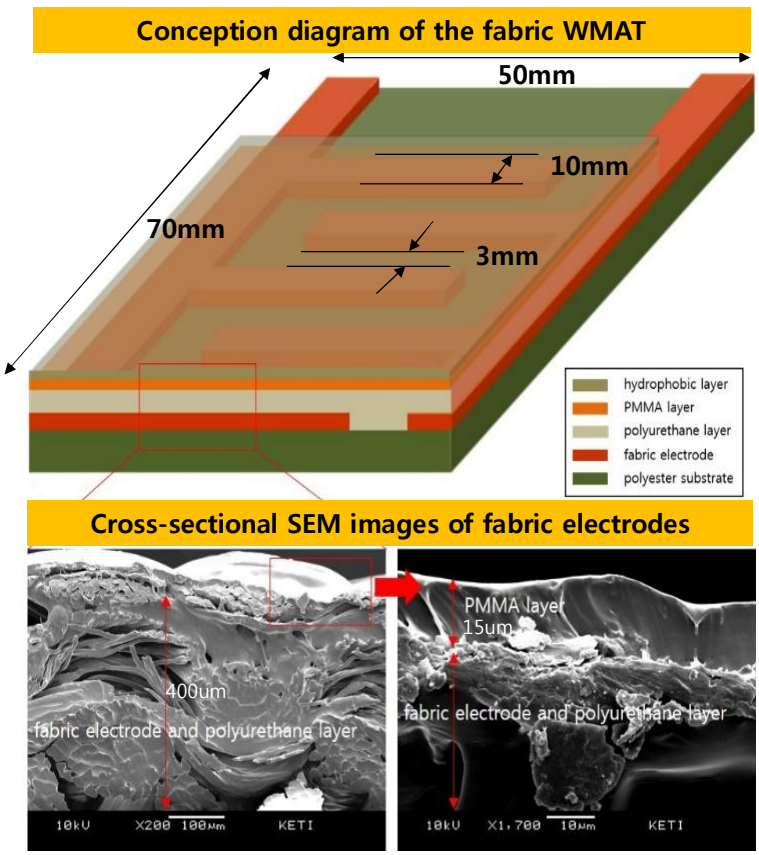

Figure 39. The conceptional diagram and cross-sectional SEM image of the Fabric WMAT.

4.3 Spray-assisted Process for Fabric WMAT

The polyurethane coating layer is needed for preventing electrical shortage owing to water absorption in the fabric electrodes.[28] First, ladder-shaped electrodes are prepared on glass or rigid substrate for convenient handling. Fabric electrodes (3M, copper plated polyester) were attached on the substrate using low tact for easy releasing from the temporary substrate. The area of ladder-shaped fabric electrodes is 7 X 5 cm and 3 mm intervals between opposite electrode with 10 mm width. Second, polyurethane solution (Flex Seal, Medline Industries, UK) was sprayed on the fabric electrode for 4 times with 40 ml at intervals of 20 minutes for room temperature curing. After polyurethane coating, polymer solutions were sprayed on the polyurethane layer 2 times with 20 minute interval with 40 ml. In this experiment, two polymers of PMMA and PVP solution were prepared and evaluated for comparison of different tribo-electric and EDL property. PMMA solution is a polymeric material resist provided by MicroChem corporate. PVP solution is a blend of Poly(4-vinylphenol), Propylene glycol monomethyl ether acetate, and Poly(melamine-coformaldehyde) methylated/butylated (Sigma Aldrich) with mass ratio 2:1:17. Finally, hydrophobic layer (ETC company, EKG-6015, Germany) was coated on the polymer layer using a spray process to prevent water droplet from sticking on the polymer energy conversion layer using the same spray process about 2 times with 20 minute interval with 40 ml. After all spray coating processes, fabric WMAT was detached from the glass substrate physically and then

attached on the final surface, for example, umbrella surface using spray adhesive (super 77, 3M, USA) shown in Figure 40. Every dry process after individual spray step was conducted at room temperature for 20 minutes. Spray equipment was commercial spray gun (LPH-80, ANEST IWATA, Italy) with nozzle size of 0.8 mm and pressure of 0.1 MPa. The distance between spray nozzle and substrate is 1 meter. Generally, fabric material is not compatible for electronics because of their entangled and uneven structure, especially for contact with water droplet.[29,30] Electronic devices, including energy harvesting device generally have a moisture vulnerability.[31] Using the fabric material for the energy harvesting device, its mesh structure must be filled with flexible and stretchable polymer material having good insulation and planarization characteristics. Polyurethane is a good material owing to its good solubility and coating property with spray process on the copper plated fabric electrodes.[32,33] Figure 41 showed SEM images of morphology change of polyurethane layer according to a repetition of spray coating process. Referring to Figure 42 of energy dispersive spectroscopy system (EDS, Oxford instrument) results indicate that a copper element is not observed on the polyurethane layer after 4 times coating process. After polyurethane spray process, we found its good insulation and waterproof characteristic between fabric electrodes and water droplets shown in Figure 42 inset image. Polyurethane layer showed good waterproof feasibility to prevent water absorption on the fabric electrode. The main principle of our fabric WMAT is based on EDL

and electrification between energy conversion layer of polymer and water droplet.

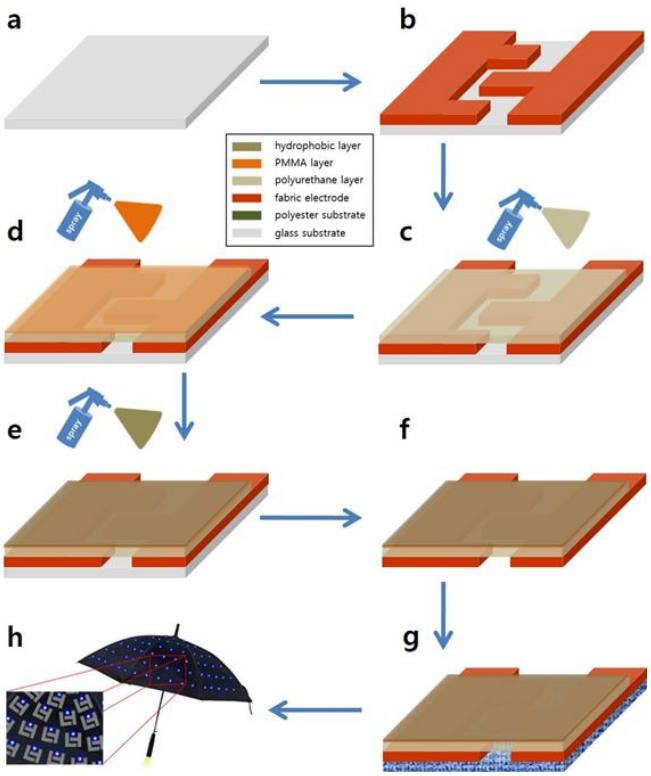

Figure 40. Spray-assisted process for fabric materials.

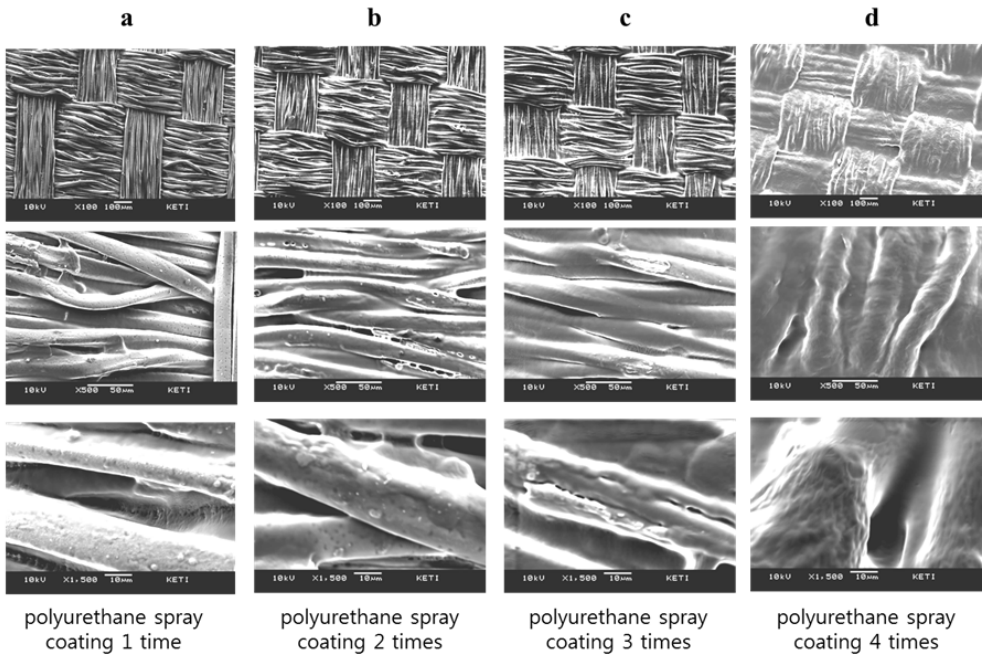

Figure 41. SEM images of morphology change of polyurethane layer according to repetition of spray coating process.

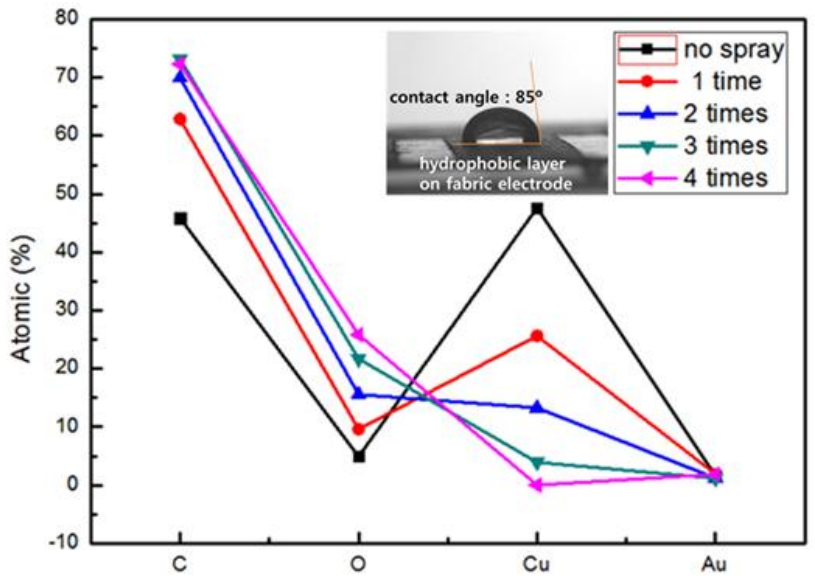

Figure 42. Energy dispersive spectroscopy system analysis result after spray coating process and waterproof characteristic of the fabric WMAT.

4.4. Electrical Property and Stability

In our previous work, we reported the polymer layer showed a permanent polarization characteristic owing to their asymmetrical molecular structure. When water droplet contacts with polymer layer, an EDL is formed at the interface although water molecules are electrically neutral.[34] The negatively induced charges of the polymer layer pull the counter ions of water droplets. Water molecules influenced by the intrinsic polarity of the polymer layer, were arranged on the interface of water droplet-polymer layer when liquid was placed on a solid surface.[35] Referring to Figure 43, overlapping area between water droplets and each electrode is changed according to the flowing of the water droplet from the upper electrode to lower electrode. Here, water droplet-electrode capacitance at time t is expressed as

$$C_u = \varepsilon A_u(t)/d \quad (1)$$

on the upper electrode,

$$C_l = \varepsilon A_l(t)/d \quad (2)$$

on the lower electrode, where ε is the permittivity of the dielectric layer, respectively. Au and A_l are overlapping area of water droplet with upper electrode and lower electrode. So variable capacitance between each electrode and water droplet is defined as

$$C_u \times C_l/(C_u + C_l) \quad (3)$$

and its maximum value is obtained when $C_u = C_l$ considering edge field effect.[36] Total capacitance is $C_t = C_v + C_e$ where C_e is

capacitance between upper and lower electrode. In our system, C_e has very tiny value so negligible. When the water droplets are ejected on the fabric WMAT substrate tilted with angle of 45° using a syringe pump (Legato 200, KdScientific Inc.), negatively charged polymer layer attracts the positive charges of water droplet at the interface owing to the electrical double layer phenomenon and positively charged water droplet passing through the upper electrode begins to overlap with the lower electrode. When a water droplet starts to overlap from the upper electrode to the lower electrode, negative charges of the lower electrode move to the upper electrode. The flow of negative charges shows the maximum value when Au and A_l is same and then dwindle away into nothing in proportion to overlap area. This generation of electricity is effective on condition that water droplet and both electrodes are overlapped at the same time as we mentioned above formula of variable capacitance. Both capacitances C_u, C_l play major roles in making the electrical potential variation and inducing charge flowing between electrodes. In this experiment, we made a comparison PVP with PMMA as an energy conversion layer having different triboelectric series and EDL properties to verify the electrical output characteristics. The output voltage and current were detected by using digital multi-meter (NI 4070, National Instruments). Voltmeter or ammeter was connected directly to the electrodes to detect electric signals. Applying the PVP energy conversion layer resulted 3 V, 10 μA of peak to peak voltage and current shown in Figure 44. In the PMMA experimental, output

peak to peak of voltage and current were 7 V and 40 μA shown in Figure 45, which were enough to turn on a green LED. PMMA energy conversion layer showed better EDL results than PVP layer. The reason of difference of electrical output of two dielectric materials is inferred from relationship of critical surface tension. Table 3 shows the critical surface tension and contact angle with water for various polymers. The lower critical surface tension brings to the higher contact angle with water. The critical surface tension of PMMA is lower than that of PVP. The high contact angle of PMMA have a possibility to play major role of excellent electrical output compare to PVP. Supplemental experiment is performed to verify the effect of the critical surface tension using fluorinated ethylene propylene (FEP) shown in Figure 46. The electrical output of final achievement showed improved voltage and current value compare to our previous flowing type WMAT. To obtain more accurate electrical output data, the impact point of water droplets on the surface of fabric WMAT is fixed. Finally, we demonstrated the situation of rainy days using fabric WMAT embedded umbrella and verified this umbrella had a function of self-lighting characteristics with only one water droplet shown in Figure 47. We transferred final fabric WMAT from the surface of the glass to outside of umbrella after all processes and then attached the each fabric WMAT on the surface of umbrella using spray type adhesives with elastic characteristics. Fabric WMAT embedded umbrella shows the peak to peak power of about 240 μW on average, which were enough to turn on a green

LED. Figure 48 and 49 showed the results of bending reputation test with using bending machine. For effective application for wearable device, bending ratio was fixed at 10 mm for 1,000 times. After 1,000 times bending, peak to peak power was maintained without dramatic change owing to all flexible materials of fabric based.

	Polymer name	Critical surface tension in mJ/m^2	Contact angle with water
1	Fluorinated ethylene propylene (FEP)	19.1	108.5
2	Polydimethylsiloxane (PDMS)	20.1	107.2
3	Polyvinylidene fluoride (PVDF)	31.6	89
4	Polymethyl methacrylate (PMMA)	37.5	70.9
5	Epoxies	44.5	76.3
6	Poly 4 vinylphenol (PVP)	57.4	62.2

Table 3. The critical surface tension and contact angle with water for various polymers.

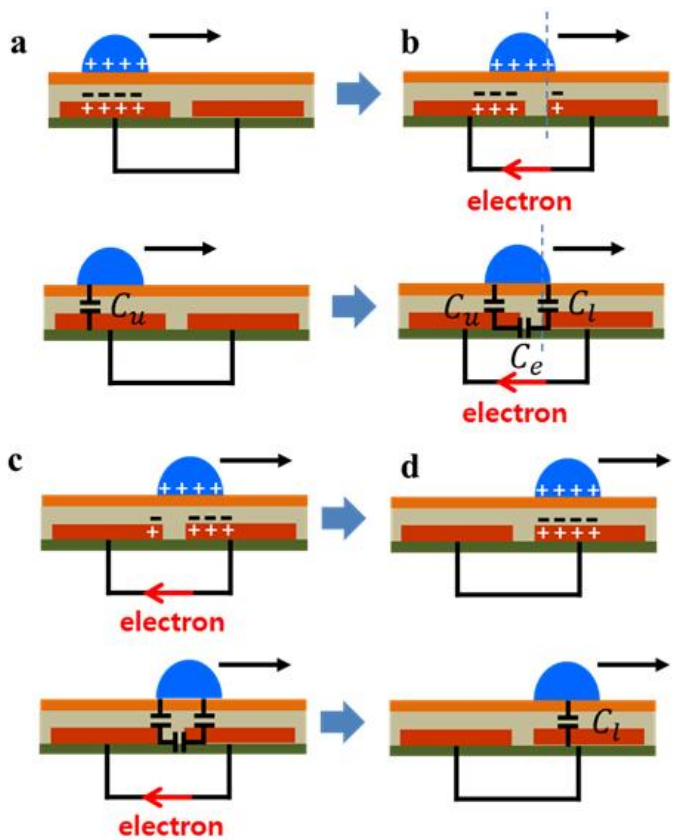

Figure 43. The fundamental operation principle of fabric WMAT.

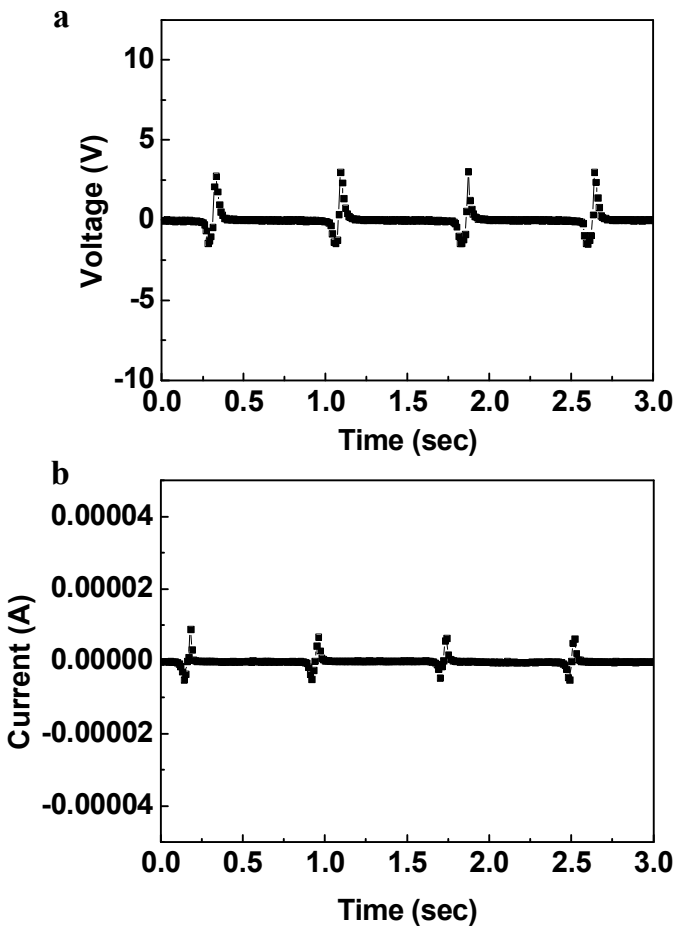

Figure 44. The measured output voltage (a) and current (b) of pushing type farbic WMAT using PVP as a dielectric layer.

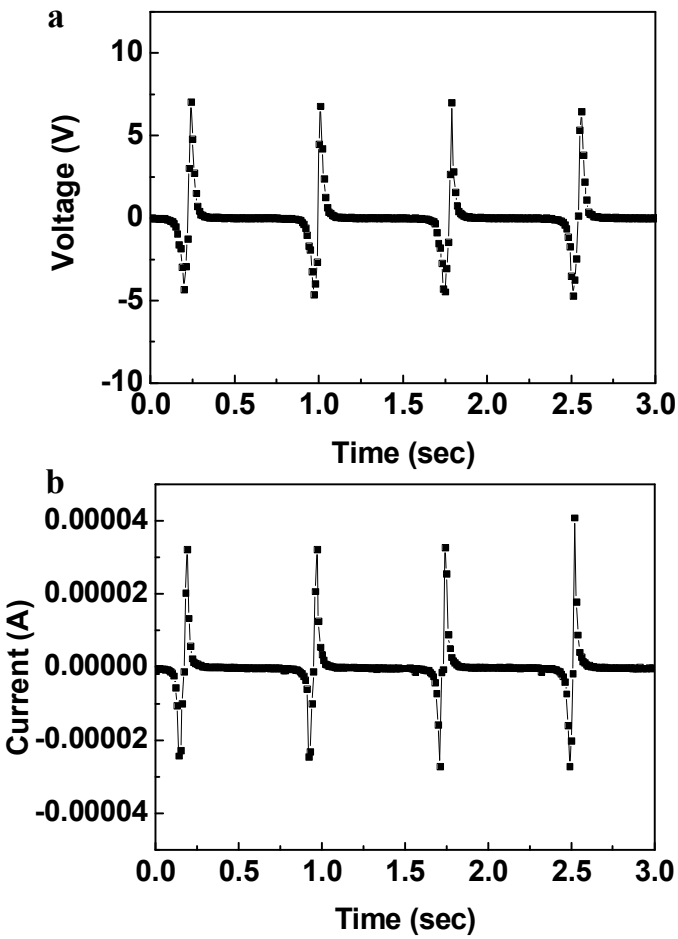

Figure 45. The measured output voltage (a) and current (b) of pushing type farbic WMAT using PMMA as a dielectric layer.

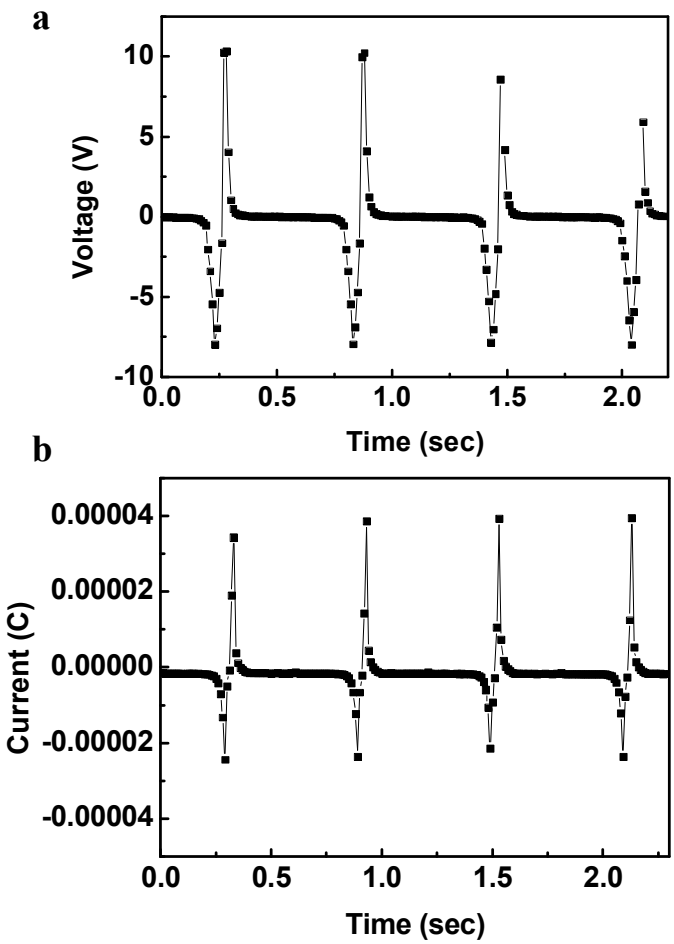

Figure 46. The measured output voltage (a) and current (b) of pushing type fabric WMAT using FEP as a dielectric layer.

Figure 47. Demonstration images of the fabric WMAT for umbrella application. Left inset image is lighting green LED when water droplet is fallen and right inset image is fabric WMAT embedded umbrella.

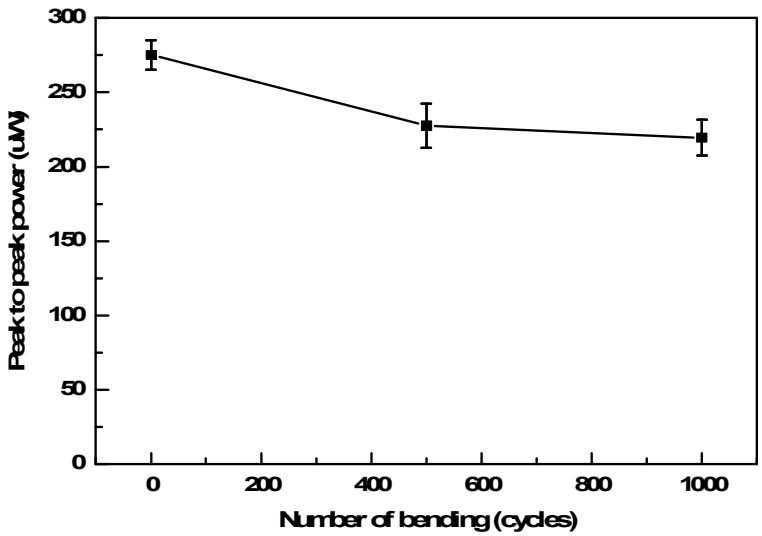

Figure 48. The results of bending reputation tests by using bending machine.

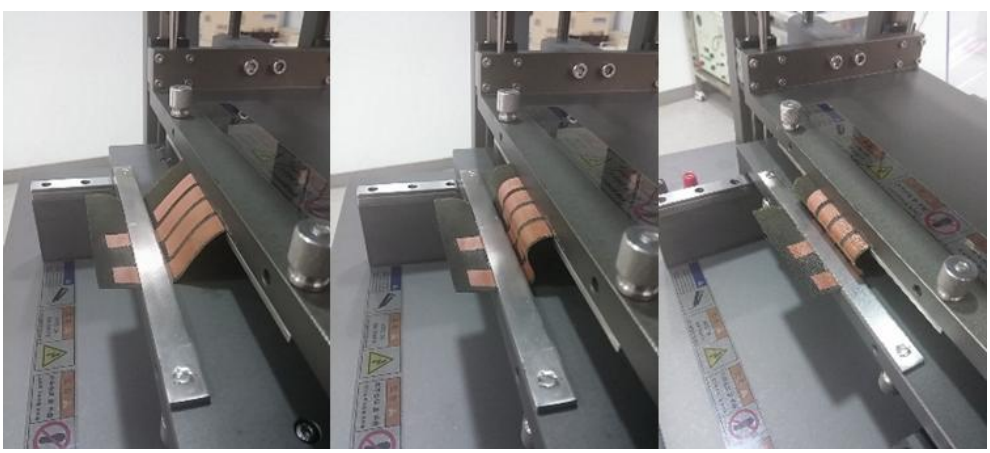

Figure 49. Bending test procedure and bending machine.

4.5 Conclusions

In summary, we successfully demonstrated self-powered lighting device operated by the fabric WMAT which generates electricity using water droplet. The core technology of this innovative device is based on the electrification and EDL theory and phenomena. In our experiment, we designed simple structure and inexpensive process not complex equipment but spray coating process using polymer solutions. Generally, fabric material is not compatible for electronics because of their entangled and uneven structure, especially for contact with water droplet. But we achieved fabric WMAT which showed good self-powered lighting characteristics through the material optimization and newly adopted spray process. In this paper, core materials for electrification and EDL to generate the electricity are PVP and PMMA energy conversion layers. Even though, various energy conversion layers are not attempted owing to suitability of spray process, we found out polyurethane-PMMA layer showed significant electrical output of 280 μW with peak to peak power. Additionally, our fabric WMAT presented good bending reputation test results essential for application of wearable device. The fabric WMAT has a good potential of self-powered wearable device for human safety supplies, sensors and rain related applications using natural water motion.

- Our fabric water motion active transducer (WMAT) has an advantage of flexible, stretchable, wearable feasibility and an excellent output using natural water motion including unfavorable environment unable to apply the general energy harvesting device.

- In this paper, we succeeded in generating an electrical energy with peak to peak power of 280 μW using a 30 μl of water droplet with the fabric WMAT device of 70 mm X 50 mm dimension.

- We specially carried out the spray coating and transfer processes instead of conventional spin coating process on fabric materials to overcome the limitation of its uneven morphology, porous and deformable assembly.

- Additionally, our fabric WMAT presented good bending reputation test results essential for application of wearable device. The fabric WMAT has a good potential of self-powered wearable device for human safety supplies, sensors and rain related applications using natural water motion.

4.6 References

1 Zeng, W, Shu, L, Li, Q, Chen, S, Wang, F, & Tao, X. M, "Fiber based wearable electronics: a review of materials, fabrication, devices, and applications", Adv Mater, 26(31), 2014, 5310-5336.

2 Jost, K, Stenger, D, Perez, C. R, McDonough, J. K, Lian, K, Gogotsi, Y, & Dion, G, "Knitted and screen printed carbon-fiber supercapacitors for applications in wearable electronics", Energy Environ Sci, 6(9), 2013, 2698-2705.

3 Park, Sungmee, and Sundaresan Jayaraman, "Smart textiles: Wearable electronic systems", MRS bulletin, 28(08), 2003, 585-591.

4 Stoppa, Matteo, and Alessandro Chiolerio, "Wearable electronics and smart textiles: a critical review", Sensors, 14(7), 2014, 11957-11992.

5 Swallow, L. M, Luo, J. K, Siores, E, Patel, I, & Dodds, D, "A piezoelectric fibre composite based energy harvesting device for potential wearable applications", Smart Mater Struct, 17(2), 2008, 025017.

6 Wu, W, Bai, S, Yuan, M, Qin, Y, Wang, Z. L, & Jing, T, "Lead zirconate titanate nanowire textile nanogenerator for wearable energy-harvesting and self-powered devices", ACS nano, 6(7), 2012, 6231-6235.

7 Kudo, H, Sawada, T, Kazawa, E, Yoshida, H, Iwasaki, Y, &

Mitsubayashi, K, "A flexible and wearable glucose sensor based on functional polymers with Soft-MEMS techniques", Biosens Bioelectron, 22(4), 2006, 558-562.

8 Pantelopoulos, Alexandros, and Nikolaos G. Bourbakis, "A survey on wearable sensor-based systems for health monitoring and prognosis", IEEE Transactions on Systems, , 40(1), 2010, 1-12.

9 Chalasani, Sravanthi, and James M. Conrad, "A survey of energy harvesting sources for embedded systems", IEEE SoutheastCon, 2008.

10 Beeby, S. P, Tudor, M. J, & White, N. M, "Energy harvesting vibration sources for microsystems applications", Meas. Sci. Technol, 17(12), 2006, R175.

11 Wang, X, Gu, Y, Xiong, Z, Cui, Z, Zhang, T, "Silk-Molded Flexible, Ultrasensitive, and Highly Stable Electronic Skin for Monitoring Human Physiological Signals", Adv. Mater, 26, 2014, 1336－1342.

12 Sokolov, A. N, Tee, B. C, Bettinger, C. J, Tok, J. B. H, Bao, Z, "Chemical and Engineering Approaches to Enable Organic Field-Effect Transistors for Electronic Skin Applications", Acc. Chem. Res, 45, 2012, 361－371.

13 Kim, D. H, Lu, N, Ma, R, Kim, Y. S, Kim, R. H, Wang, S, Yu, K. J, Rogers, J, "Epidermal Electronics", Science, 333, 2011, 838－843.

14 Zeng, W, Shu, L, Li, Q, Chen, S, Wang, F, Tao, X. M,

"Fiber-Based Wearable Electronics: A Review of Materials, Fabrication, Devices, and Applications", Adv. Mater, 26, 2014, 5310－5336.

15 Lee, Jaehong, et al, "Conductive Fiber Based Ultrasensitive Textile Pressure Sensor for Wearable Electronics", Adv Mater, 27(15), 2015, 2433-2439.

16 Kim, S. J, We, J. H, Cho, B. J, "A Wearable Thermoelectric Generator Fabricated on a Glass Fabric", Energy Environ. Sci, 7, 2014, 1959－1965.

17 Zhong, J, Zhang, Y, Zhong, Q, Hu, Q, Hu, B, Wang, Z. L,Zhou, J, "Fiber-Based Generator for Wearable Electronics and Mobile Medication", ACS Nano, 8, 2014, 6273－6280.

18 Chocat, N, Lestoquoy, G, Wang, Z, Rodgers, D. M, Joannopoulos, J. D, Fink, Y, "Piezoelectric Fibers for Conformal Acoustics", Adv. Mater, 24, 2012, 5327－5332.

19 Zeng, W, Tao, X. M, Chen, S, Shang, S, Chan, H. L. W, Choy, S. H, "Highly Durable All-Fiber Nanogenerator for Mechanical Energy Harvesting", Energy Environ. Sci, 6, 2013, 2631－2638.

20 Rogers, J, "Electronics: A Diverse Printed Future", Nature 468, 2010, 177－178.

21 Yamada, T, Hayamizu, Y, Yamamoto, Y, Yomogida, Y, Izadi-Najafabadi, A, Futaba, D. N, Hata, K. A, "Stretchable Carbon Nanotube Strain Sensor for Human-Motion Detection", Nat. Nanotechnol, 6, 2011, 296－301.

22 Kwon, S. H, Park, J, Kim, W. K, Yang, Y, Lee, E, Han, C.J, Kim, Y. S, "An Effective Energy Harvesting Method from a Natural Water Motion Active Transducer", Energy Environ. Sci, 7, 2014, 3279-3283.

23 Moon, J. K, Jeong, J, Lee, D, Pak, H. K, "Electrical Power Generation by Mechanically Modulating Electrical Double Layers", Nat. Commun, 4, 2013, 1487.

24 Miljkovic, N, Preston, D. J, Enright, R, Wang, E. N, "Electrostatic Charging of Jumping Droplets", Nat. Commun, 4, 2013, 2517.

25 Lin, Z. H, Cheng, G, Li, X, Yang, P. K, Wen, X, Wang, Z. L, "A Multi Layered Interdigitative Electrodes Based Triboelectric Nanogenerator for Harvesting Hydropower", Nano Energy 15, 2015, 256-265.

26 Park, J, Yang, Y, Kwon, S. H, Kim, Y. S, "Influences of Surface and Ionic Properties on Electricity Generation of an Active Transducer Driven by Water Motion", J. Phys. Chem. Lett, 6, 2015, 745-749.

27 Yang, Y, Park, J, Kwon, S. H, Kim, Y. S, "Fluidic Active Transducer for Electricity Generation", Sci. Rep, 5, 2015, 15695.

28 Lomax, G. R, "Hydrophilic Polyurethane Coatings", J. Ind. Text, 20, 1990, 88-107.

29 Lee, Y. H, Kim, J. S, Noh, J, Lee, I, Kim, H. J, Choi, S, Seo, J, Jeon, S, Kim, T.-S, Lee, J.-Y, Choi, J. W, "Wearable

Textile Battery Rechargeable by Solar Energy", Nano Lett, 13, 2013, 5753－5761.

30 Saxena, P. K, Raut, K. G, Srinivasan, S. R, Sivaram, S, Rawat, R. S, Jain, R. K, "Polyurethane Waterproofing Coating for Building Applications", Constr Build Mater, 5, 1991, 208－210.

31 Shoujia, Z, "Brief Introduction of Development of Polyurethane Waterproof Coatings", Polyeurathane Industry, 3, 2000, 005.

32 Grahame, D. C, "The Electrical Double Layer and The Theory of Electrocapillarity", Chem. Rev, 41, 1947, 441－501.

33 Li, D, "Electrokinetics in Microfluidics", Elsevier Academic Press, 2004, Chapter 2, 10.

34 Parsons, R, "The Electrical Double Layer: Recent Experimental and Theoretical Developments", Chem. Rev, 90, 1990, 813－826.

35 Yin, J, Li, X, Yu, J, Zhang, Z, Zhou, J, Guo, W, "Generating Electricity by Moving a Droplet of Ionic Liquid along Graphene", Nat. Nanotechnol, 9, 2014, 378－383.

36 Yang, Z, Halvorsen, E, Dong, T, "Power Generation from Conductive Droplet Sliding on Electret film", Appl. Phys. Lett, 100, 2012, 213905.

Chapter 5. Conclusion

This paper is about the energy harvesting method to use natural phenomenon such as water flow, water drain and rainfall caused by gravity for autonomous system without any external electrical source. I concentrated my every efforts to find out the practical design to generate the electricity with easy and not expensive process without vacuum equipment. In first part, I studied about the basic water motion active transducer differ from previous energy harvesting device using liquid. In this experiment, I proposed a new concept to generate electricity from water's natural motion without any cumbersome conversion parts or external sources. I found that the overlap area variation between the water and the dielectric layer can effectively induce the variation of electric charges, and then easily generate electricity. The suggested hydroelectric energy harvester which is based on the difference of overlap areas variation between water and electrodes has a simple structure: substrate including the patterned transparent electrodes, poly-4-vinyl phenol (PVP) dielectric layers, and hydrophobic layers. This simple structure in the new hydroelectric energy harvester makes it possible to easily produce electricity from various natural water phenomena in our surroundings, such as rain, rivers, and even sea waves. I achieved electrical power generation of 3.1 V and 5.3 μA from the flowing of the only one tap-water droplet of 30 μL, and successfully turned on light emitting diodes (LED) with natural mimetic water movements, via the

suggested hydroelectric energy harvester. As these new hydroelectric energy harvesters can easily be extended to scale-up power production by the simple stack or array process and have a wide applicability range in hydroelectric generation.

My next interest of research was fabric-based water motion active transducer. Here, I proposed fabric-based water motion active transducer (WMAT) which has an excellent electrical output using natural water motion like rain for innovative umbrella of self-powered lighting. In this research, I studied the principle of electricity generation from electrical double layer (EDL) between newly adopted fabric electrode and polyurethane-poly methyl-methacrylate (PMMA) layer. Furthermore, I specially carried out spray coating and transfer process with fabric based material to overcome the limitation of spin coating and lithography process of high temperature and chemical treatment. I verified polyurethane-PMMA layer with spray coating process are effective dielectric layer and energy conversion layer on the fabric substrate. To achieve final demonstration, fabric WMAT was detached from glass substrate after core process and was attached to polyester substrate of umbrella surface using transfer process. Unlike the other complex and sensitive energy harvesting devices, our fabric WMAT has an advantage of physical bending and folding characteristic because all materials are flexible and foldable fabrics. Fabric WMAT has a similar structure with our previous glass-based WMAT but core material is changed suitable for fabric-based process. The main principle of our fabric WMAT is

based on electrical double layer (EDL) between PMMA energy conversion layer and water droplet. Water droplet on energy conversion layer is charged with positive polarity due to the asymmetric molecular structure of PMMA with negative polarity. Charged water droplet induces capacitance variation with each electrode and contributes generating electricity. Finally, we realized fabric-based WMAT using spray coating and transfer process of easy and cheap without photo-lithography process of high cost. I achieved the electricity with a peak voltage of 9 V and peak current of 50 μA enough to turn on a green LED using a water droplet of about 30 μL. The fabric WMAT has a good potential of self-powered wearable device for human safety supplies, sensors, and rain-related applications using natural water motion.

요 약 (국문초록)
물의 움직임을 이용하는 능동형 트랜스듀서의 에너지 하베스팅 적용 연구

본 논문은 물방울의 움직임을 이용하여 전기를 발생시키는 에너지 하베스팅에 대한 연구이다. 흘러내리는 물이나 빗방울 또는 파도나 강물의 움직임을 이용한 에너지 하베스팅 연구를 통해 전원이나 배터리가 필요 없는 자주적인 장치나 더 나아가 전통적인 터빈의 회전을 통해 기계적 에너지를 전기적 에너지로 변환시키는 형태를 벗어나 단순히 정전용량 변화를 통한 에너지 획득을 가능케 하는데 목적이 있다. 기존의 액체를 이용하는 정전용량 변화 기술의 경우 다음 2가지 한계점이 있었다. 첫째는 수은이나 갈린스탄과 같은 환경에 유해한 전도성 액체를 사용하는 점이며, 둘째는 그 장치의 복잡함으로 인해 제작이나 유지에 많은 비용이 발생하는 점이다. 물론 피에조 효과나 마찰 효과를 이용해 물의 움직임을 전기로 변화하는 연구도 활발하다. 하지만 피에조의 경우 대부분의 중요 물질이 세라믹과 같은 무기물로 외부 충격이나 압력에 취약한 점이 있으며, 마찰 효과의 경우 계속적인 마찰로 인해 장치 자체의 문제점이 발생하거나 전기발생 효과가 떨어지는 단점이 있다. 본 연구는 이러한 기존의 에너지 하베스팅 기술의 단점을 극복하고 실용적, 경제적으로 사용 가능한 장치 구현을 위해 다음의 2가지 연구를 진행하였다. 첫째는 물의 움직임, 접촉을 이용한 에너지 하베스팅 장치의 개발이다. 일반적인 폴리머들은 물리적인 구조의 비대칭성 때문에 물과 접촉 시 표면 전위가 음전위로 대전된다. 물은 반대로 양전위로 대전된다. 이것은 전기 이중층에 기초한 현상으로 대전되는 범위는 유전체와 물의 접촉면적 변화에 관계있으며, 두개 이상의 전극위에 유전체를 형성하여 물과의 접촉 면적

변화를 관찰하면 용량변화가 발생함을 알 수 있었고 저항과 연결 시 전기 에너지를 발생시킬 수 있음을 확인하였다. 이러한 현상을 기초로 물방울을 누르는 형태, 물방울의 흐름을 이용하는 형태, 물에 본 소자를 Dipping하는 형태로 실험을 진행하였다. 물의 흐름을 이용하는 소자에서는 물방울 30 μL를 이용하여 3.1 V and 5.3 μA의 AC형태의 피크 펄스를 얻었으며 이를 통해 녹색 LED를 점등시킬 수 있었다. 본 Water Motion Active Transducer (WMAT) 소자는 Indium Tin Oxide (ITO) 전극과 Poly-4-vinyl phenol (PVP) 유전체, Hydrophobic Layer로 구성되어 있으며 물의 전자를 유도시키는 PVP의 경우 투명하고 전극 및 소수성 물질과의 접착 특성도 우수하였다. WMAT의 대부분의 공정은 진공 공정이 아닌 솔루션 공정으로 진행하였으며 이를 통해 다양한 물의 움직임이 있는 분야에 에너지 하베스팅 소자로 사용될 것을 기대한다. 두 번째 연구는 기존의 WMAT 소자를 패브릭 소재를 이용하여 구현하는 것이었다. 일반적인 패브릭 소재는 필름이나 유리 기판처럼 스핀 코팅 공정이 어렵다. 이를 극복하기 위해 본 연구에서는 스프레이 코팅 공정을 진행하였다. 폴리우레탄의 경우 스프레이 공정에 적합하며 방수 특성이 좋은 물질로 알려져 있다. 패브릭 WMAT의 경우 기존 WMAT와 물질 및 공정을 달리해야 했는데, 물질은 소자의 전기적 방수 특성 향상을 위해 폴리우레탄을 추가하였으며, 발생 전압 및 전류 향상을 위해 poly methyl-methacrylate (PMMA)를 유전체로 적용하여 진행하였다. 공정의 편의성을 위해 Transfer 공정을 진행하였다. 유리기판과 같은 Rigid한 기판을 이용하여 스프레이 코팅공정을 진행한 뒤 최종 응용제품에 옮겨 붙이는 공정을 고려하여 Adhesive를 결정해야 한다. 폴리우레탄-PMMA 유전층 적용 패브릭 WMAT 소자는 물방울 30 μL를 이용하여 9 V and 50 μA의 AC형태의 피크 전력을 발생시켰으며 이는 기존

WMAT의 전기적 특성보다 우수한 결과였다.

결론적으로 본 WMAT를 개발을 통해 외부의 전원공급이 필요했던 기존의 액체를 이용한 에너지 하베스팅 장치의 단점을 극복하고 외부 전원 공급이 필요 없으며 친환경 재료인 물을 이용하는 에너지 하베스팅 장치를 개발하였다. 물과 유전층 사이에 발생되는 전기 이중층 현상을 전기로 변환시킬 수 있는 구조를 설계하였으며 이를 통해 다양한 물흐름 전기 에너지를 발생시켰다. 더 나아가 패브릭 형태의 WMAT를 고안하여 기존 에너지 하베스팅 장치의 물에 대한 취약성을 극복하였으며 이를 통해 더 많은 응용분야에 적용할 수 있게 되었다.

주요어 : 가변용량, 에너지 하베스팅, 자가발전 장치, 능동 트랜스듀서, 물움직임, 에너지 변환

학 번 : 2012-30691